Modelling and identification of the CFT-transposer robot

Modelling and Identification of the CFT-Transposer Robot

A. Rodriguez-Angeles, D. Lizarraga,
H. Nijmeijer, and H. A. van Essen

Report No. WFW 2002.52

Eindhoven, September 2002

Eindhoven University of Technology
Department of Mechanical Engineering
Section Dynamics and Control

Modelling and Identification of the CFT-Transposer Robot
Dynamics and Control Technology report number: WFW 2002.52

A. Rodriguez-Angeles, D. Lizarraga, H. Nijmeijer, and H. A. van Essen

Contents

1 Introduction

The CFT robot is a Cartesian robot with a basic elbow configuration, designed and built by Philips Centre for Manufacturing Technology (CFT). It consists of a two links arm which is placed on a rotating base, and has a passively actuated tool connected at the end of the outer link. The CFT robot is a pick and place industrial robot used for assembling. It has 4 degrees of freedom in the Cartesian space and 7 degrees of freedom in the joint space, and is actuated by 4 DC brushless servomotors.
The 4 Cartesian degrees of freedom are rotation, up and down, forward and backward movement of the arm, forward and backward of the whole robot, see Figure 1. The robot is equipped with encoders attached to the shaft of the motors with a resolution of 2000 PPR, what results in an accuracy of ± 0.5 [mm] in all motion directions. The tool connected at the end of the outer link is a kinematically constrained planar support. The tool is passively actuated and designed to keep a horizontal plane at all time.
Although the shaft of the motors and the corresponding links are connected by means of belts, the servomotor-link pair proved to be stiff enough to be considered as a rigid joint.

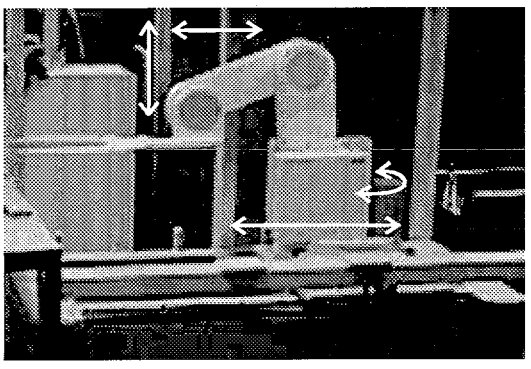

Figure 1: The CFT-transposer robot

A mathematical model for the CFT robot is needed for different reasons, including simulation purposes and model based control design. A full mathematical description of the robot includes the kinematic and dynamic models, and a set of physical parameters of the robot, such as masses, inertias, friction coefficients. The kinematic model relates the position and orientation of the end-effector and the joint coordinates. The dynamic model relates the joint coordinates with the applied torques. The physical parameters involved in the models have to be identified or estimated since most of them cannot be measured or known a priori.
In this report, a general and straightforward modelling approach is described. This approach can be easily implemented in a symbolic manipulation package, and results in an explicit model. The approach is based on a rigid body model, that is derived using the Denavit-Hartenberg convention to describe the kinematics in a systematic manner [5]. Based on the direct kinematic model the Euler-Lagrange approach is used to derive the dynamics [9], [10].
For estimation of the physical parameters two methods are considered, namely extended Kalman filters and the standard linear least square estimation method, similar to the work presented in [8]. The first method is based on an extension of the dynamic model by the physical parameters being considered as extended states. The second method is based on a linear parametrization of the dynamical model into a regressor matrix, which is function of measurements and known parameters, and a vector of unknown parameters. For identification purposes a parametric excitation trajectory is designed such that an optimization criterion is fulfilled. The parametric excitation trajectory is a finite Fourier series that allows specification of the bandwidth of the excitation trajectory. The optimization criterion is the uncertainty on the estimated parameters or a upper bound for it.
The considered approaches for modelling and identification are designed for the joint space. However as mentioned the CFT robot has a different number of degrees of freedom in the Cartesian and in the joint space. Therefore both models in Cartesian and joint space must be obtained and the relation between them has to be established.
Throughout this report all the units are in SI and the angles are in radians. Also standard notation is used, in particular, vector norms are Euclidean, and for matrices the induced norm

$\|A\| = \sqrt{\lambda_{\max}(A^T A)}$ is employed, with $\lambda_{\max}(\cdot)$ the maximum eigenvalue. Moreover, for any positive definite matrix A we denote by A_m and A_M its minimum and maximum eigenvalue respectively.

2 Modelling and identification of robotic systems

This section presents general approaches to compute the joint space kinematic and dynamic model of a robot manipulator. The kinematic model formulation is based on a rigid body model, that is derived using the Denavit-Hartenberg convention to describe the kinematics in a systematic manner [5]. Based on the direct kinematic model the Euler-Lagrange approach is used to derive the dynamics [9], [10].
The presented approaches for kinematic and dynamic models have been implemented in a symbolic manipulation package (Maple), and result in explicit models for the CFT-robot. The resulting kinematic and dynamic models are presented in Sections 4.1 and 4.2 respectively.

2.1 Kinematics

The first step in modelling a manipulator is formulating the kinematics. It is the relation between the joint coordinate space and the position and orientation of each link with respect to a reference frame.
A convenient way to represent the kinematic relationships is by using vector-matrix description. Then the direct kinematic problem is to find a transformation matrix that relates a body-attached coordinate frame to the reference coordinate frame.
To include both rotation and translation (and if necessary, scaling), a 4×4 homogeneous transformation matrix can be used [5]. This transformation matrix maps an augmented position vector $p = [\ p_x \quad p_y \quad p_z \quad 1\ ]^T$ from one coordinate system to another one. In robotics this homogeneous transformation is given by

$$T = \begin{bmatrix} 3 \times 3 \text{ rotation matrix} & 3 \times 1 \text{ translation vector} \\ 0 \quad 0 \quad 0 & 1 \end{bmatrix} \tag{1}$$

A minimum of four parameters is needed to describe the above transformation: two distances, a and d, and two angles, α and q. The definition of the parameters a, d, α, and q depend on how the frames attached to the link are assigned, and there is quite some freedom in how to assign those frames (see for instance [5] and [10]).
Along the proposed approaches we particularly consider the convention presented in [5]. This convention is as follows. The $z-$axis of frame $\{i\}$, denoted by z_i, is coincident with the joint axis i. The origin of frame $\{i\}$ is located where the a_i perpendicular intersects the joint i axis. The x_i-axis points along a_i in the direction from joint i to joint $i+1$. The axis y_i is then chosen according to the right hand rule. Figure 2 shows the location of frames $\{i-1\}$ and $\{i\}$ for a general manipulator.
If the frames attached to the links have been assigned according to the above convention, then the link parameters can be defined according to the Denavit-Hartenberg convention as follows

a_i = the distance from z_i to z_{i+1} measured along x_i;
α_i = the angle between z_i and z_{i+1} measured about x_i;
d_i = the distance from x_{i-1} to x_i measured along z_i;
q_i = the angle between x_{i-1} and x_i measured about z_i;

For any given robot, the homogeneous transformation (1) is function of only one variable, the other three parameters being fixed by mechanical design. After coordinate frames have been attached to each rigid link, the position and orientation of frame $\{i\}$, with respect to a previous frame $\{i-1\}$, is given by (see [5]),

$$T_i^{i-1} = \begin{bmatrix} \cos(q_i) & -\sin(q_i) & 0 & a_{i-1} \\ \sin(q_i)\cos(\alpha_{i-1}) & \cos(q_i)\cos(\alpha_{i-1}) & -\sin(\alpha_{i-1}) & -d_i \sin(\alpha_{i-1}) \\ \sin(q_i)\sin(\alpha_{i-1}) & \cos(q_i)\sin(\alpha_{i-1}) & \cos(\alpha_{i-1}) & d_i \cos(\alpha_{i-1}) \\ 0 & 0 & 0 & 1 \end{bmatrix} \tag{2}$$

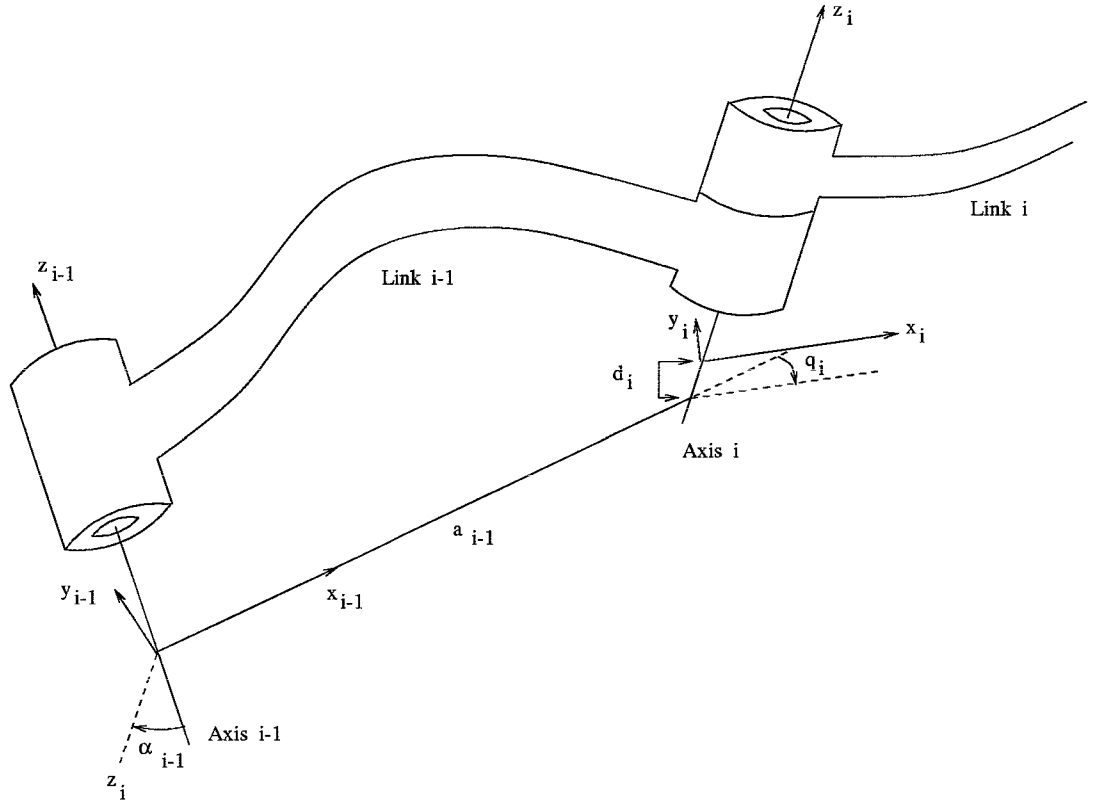

Figure 2: Link kinematic relations

For a kinematic chain the coordinate transformation T_n^0, which relates frame $\{n\}$ to frame $\{0\}$, is given by

$$T_n^0 = T_1^0 T_2^1 T_3^2 \cdots T_n^{n-1}$$

Using the above transformation, all link properties defined in their own link coordinates, can be expressed in base coordinates, e.g. the center of gravity and the link or motor inertia. Thus in terms of the reference frame at the base, the position of a point p_i on link i is given by

$$p_i^0 = T_i^0 p_i$$

with $p_i = [\ p_{xi} \quad p_{yi} \quad p_{zi} \quad 1\ ]^T$ the position vector of point p_i in frame $\{i\}$.
The proposed approach to obtain the kinematic model of a robot is applied to the CFT-robot in Section 4.1.

2.2 Dynamics

There are several approaches for deriving the dynamics of a robot manipulator, e.g. Euler-Lagrange, Newton-Euler, recursive Euler Lagrange. These methods vary greatly in computational effort and efficiency. In particular, the Euler-Lagrange approach is straightforward to compute, and from a control viewpoint results in a very convenient set of equations of the form

$$M(q)\ddot{q} + C\left(q, \dot{q}\right)\dot{q} + G(q) = \tau^\star \tag{3}$$

where $q \in \mathbb{R}^n$ is the vector of generalized coordinates or joint variables, n is the number of joints in the robot, $M(q) \in \mathbb{R}^{n \times n}$ denotes the symmetric positive definite inertia matrix, $C\left(q, \dot{q}\right)\dot{q} \in \mathbb{R}^n$ accounts for the Coriolis and centrifugal torques, $G(q) \in \mathbb{R}^n$ represents the conservative torques due to gravity, and $\tau^\star(\cdot)$ is the $n-$vector of non-conservative torques, such as input torques and friction forces.
When considering friction forces in the dynamic model (3), the non-conservative forces $\tau^\star$ can be written as

$$\tau^\star = \tau + \tau_f(\dot{q}, z) \tag{4}$$

where τ are the external torques, and $\tau_f(\dot{q}, z)$ represent the forces due to friction phenomena, z represents all the extra states defined by the dynamic friction effects.
The coefficient matrices $M(q)$, $C(q, \dot{q})$ and $G(q)$ can be determined from the Lagrange equations of motion

$$\frac{d}{dt}\frac{\partial L}{\partial \dot{q}} - \frac{\partial L}{\partial q} = \tau^{\star}$$

where the Lagrangian, denoted by L, is the difference between the kinetic (K) and potential (P) energies, i.e.

$$L = K - P$$

By using the homogeneous transformation (2), the kinetic and potential energy can be expressed for each link as follows (see [9] and [10] for an extensive formulation).

2.2.1 Kinetic energy

The kinetic energy of link i in the base coordinate frame is given by

$$K_i = \frac{1}{2}\,\mathrm{trace}\left\{\sum_{j=1}^{n}\sum_{k=1}^{n}\frac{\partial T_i^0}{\partial q_j} I_i \left(\frac{\partial T_i^0}{\partial q_k}\right)^T \dot{q}_j \dot{q}_k\right\}$$

with $I_i \in \mathbb{R}^{4\times 4}$ the inertia matrix of link i.
Therefore, the total kinetic energy of the robot can be written as

$$K = \frac{1}{2}\sum_{i=1}^{n}\mathrm{trace}\left\{\sum_{j=1}^{n}\sum_{k=1}^{n}\frac{\partial T_i^0}{\partial q_j} I_i \left(\frac{\partial T_i^0}{\partial q_k}\right)^T \dot{q}_j \dot{q}_k\right\} \tag{5}$$

The inertia matrix I_i is a constant matrix that is evaluated once for each link. It depends on the geometry and mass distribution of link i, and can be written as

$$I_i = \begin{bmatrix} \frac{-I^*_{xxi}+I^*_{yyi}+I^*_{zzi}}{2} & I_{xyi} & I_{xzi} & m_i x_{ci} \\ I_{xyi} & \frac{I^*_{xxi}-I^*_{yyi}+I^*_{zzi}}{2} & I_{yzi} & m_i y_{ci} \\ I_{yzi} & I_{xzi} & \frac{I^*_{xxi}+I^*_{yyi}-I^*_{zzi}}{2} & m_i z_{ci} \\ m_i x_{ci} & m_i y_{ci} & m_i z_{ci} & m_i \end{bmatrix}$$

where I^*_{xxi}, I^*_{yyi}, I^*_{zzi} are the moments of inertia, I_{xyi}, I_{xzi}, I_{yzi} denote the cross-products of inertia, $m_i x_{ci}$, $m_i y_{ci}$, $m_i z_{ci}$ are the first moments, m_i is the total mass of link i, and $p_{ci} = \begin{bmatrix} x_{ci} & y_{ci} & z_{ci} \end{bmatrix}^T$ represents the position of the center of gravity of link i in the frame $\{i\}$.
The inertia matrix I_i is determined by p_{ci}, that is referred to the frame $\{i\}$. Therefore, there is a homogeneous matrix T^i_{ci}, of the form (1), associated with the center of gravity. T^i_{ci} relates a coordinate frame $\{c_i\}$ with origin at the center of gravity of link i to the frame $\{i\}$ located at the base of link i, and it is given by

$$T^i_{ci} = \begin{bmatrix} I_{3\times 3} & p_{ci} \\ 0_{1\times 3} & 1 \end{bmatrix}$$

with $I_{3\times 3}$ the identity matrix. Thus the frame $\{c_i\}$ is related to the base frame $\{0\}$ by the homogeneous transformation

$$T^0_{ci} = T^0_i T^i_{ci} \tag{6}$$

In terms of the homogeneous transformation T^0_{ci}, $i = 1, \ldots, n$, the total kinetic energy of the robot (5) can be written as

$$K = \frac{1}{2}\sum_{i=1}^{n}\mathrm{trace}\left\{\sum_{j=1}^{n}\sum_{k=1}^{n}\frac{\partial T^0_{ci}}{\partial q_j} I_{ci} \left(\frac{\partial T^0_{ci}}{\partial q_k}\right)^T \dot{q}_j \dot{q}_k\right\} \tag{7}$$

with the inertia matrix I_{ci} given by

$$I_{ci} = \begin{bmatrix} \frac{-I^*_{xxi}+I^*_{yyi}+I^*_{zzi}}{2} & I_{xyi} & I_{xzi} & 0 \\ I_{xyi} & \frac{I^*_{xxi}-I^*_{yyi}+I^*_{zzi}}{2} & I_{yzi} & 0 \\ I_{yzi} & I_{xzi} & \frac{I^*_{xxi}+I^*_{yyi}-I^*_{zzi}}{2} & 0 \\ 0 & 0 & 0 & m_i \end{bmatrix} \tag{8}$$

2.2.2 Potential energy

Expressed in the base coordinate frame the potential energy P_i of link i is given by

$$P_i = -m_i g^T T_i^0 \begin{bmatrix} p_{ci} \\ 1 \end{bmatrix}$$

with m_i the total mass of link i, $p_{ci} = \begin{bmatrix} x_{ci} & y_{ci} & z_{ci} \end{bmatrix}^T$ the position of the center of gravity of link i in frame $\{i\}$, and $g = \begin{bmatrix} g_x & g_y & g_z & 0 \end{bmatrix}^T$ the gravity vector expressed in base coordinates. Therefore, the total potential energy of the robot is

$$P = -\sum_{i=1}^{n} m_i g^T T_i^0 \begin{bmatrix} p_{ci} \\ 1 \end{bmatrix} \tag{9}$$

2.2.3 Friction forces

The friction forces $\tau_f(\dot{q}, z) \in \mathbb{R}^n$ in the dynamic model (3) are in general of the form

$$\tau_f(\dot{q}, z) = F_s(\dot{q}) + F_d(\dot{q}, z) \tag{10}$$

with $F_s(\dot{q})$ the forces due to static friction and $F_d(\dot{q}, z)$ a model for dynamic friction phenomena, with z the extra states defined by the dynamic friction effects.
Dynamic friction models $F_d(\dot{q}, z)$ are useful to describe stick-slip phenomena and presliding displacements, such as elastic and plastic deformations of the asperity junctions before macroscopic sliding. In dynamic friction models the idea is to introduce extra state variables (or internal states), here denoted by z, that determine the level of friction in addition to velocity. The evolution in time of the extra state z is governed by a set of differential equations.
Static friction models $F_s(\dot{q})$ are characterized by the absence of internal states, i.e. they do not increase the order of the system. Static friction phenomena include Coulomb, viscous and Stribeck effects. The static friction models are static maps from the relative velocity between the two contact surfaces to the friction force.
In general dynamic friction models are more complicated than static models. At very low velocities dynamic friction greatly affects the performance of the systems. However the use of dynamic friction models is not justified for medium and high velocities. Therefore only static friction models are considered throughout this report, thus it is assumed that $F_d(\dot{q}, z) = 0$ in (10), such that the friction forces in the non-conservative torques $\tau^\star$ in (4) reduces to

$$\tau^\star = \tau + \tau_f = \tau + F_s(\dot{q}) \tag{11}$$

Since friction is a local effect, it may be assumed that the static friction forces $F_s(\dot{q})$ are uncoupled among the joints, so that, $F_s(\dot{q})$ can be written as

$$F_s(\dot{q}) = \begin{bmatrix} f_{s,1}(\dot{q}_1) & f_{s,2}(\dot{q}_2) & \cdots & f_{s,n}(\dot{q}_n) \end{bmatrix}^T \tag{12}$$

with $f_{s,i}(\dot{q}_i)$ scalar functions that can be determined for any given robot.
One of the largest difficulties on static models is the discontinuity that the Coulomb friction represents. The discontinuity at zero velocity may lead to non-uniqueness of the solution of the robot dynamics (3), and numerical problems if such a model is used in simulations. An alternative way to deal with the Coulomb discontinuity is to use approximations based on tangent or exponential functions. In this report we considered an approximation based on exponential functions as follows. Consider the friction model proposed in [7], then the torque $\tau_f(\dot{q}) = F_s(\dot{q})$ due to static friction effects is modelled as

$$F_s(\dot{q}) = B_v \dot{q} + B_{f1}\left(1 - \frac{2}{1 + e^{2w_1\dot{q}}}\right) + B_{f2}\left(1 - \frac{2}{1 + e^{2w_2\dot{q}}}\right) \tag{13}$$

where B_v represents the diagonal viscous friction coefficient matrix and the remaining terms approximate the Coulomb and Stribeck friction effects.
Note that the parameters B_v, B_{f1}, and B_{f2} appear in a linear way in the model (13). However the parameters w_1 and w_2 are argument of the exponential function, thus they cannot be included

in a linear parametrization of (13). This fact complicates the parameter estimation stage, and it is the reason why extended Kalman filters are considered for parameters estimation, besides the linear least square methods.
Other models for static and/or dynamic friction can be assumed, see [1], [2], [3]. The use of other friction models different from (13) in the CFT-robot dynamics is left as an open issue for further extension of the model presented here.

Remark 1 *In the friction model (13) it is assumed that the friction is symmetric, and it is only function of the joint velocity $\dot{q}$, although in many robot applications it turns out that friction also exhibits some dependence on the joint position q. It is also assumed that the friction effects in the robot are decoupled with respect to the joint velocities, i.e. the friction effects on the i-th joint only depend on the joint velocity $\dot{q}_i$, see (12).*

2.2.4 Componentwise analysis of the robot dynamics

From (7) and (9), the Lagrangian of a robot can be written as

$$L = \frac{1}{2}\sum_{i=1}^{n} \text{trace}\left\{\sum_{j=1}^{n}\sum_{k=1}^{n} \frac{\partial T_{ci}^0}{\partial q_j} I_{ci} \left(\frac{\partial T_{ci}^0}{\partial q_k}\right)^T \dot{q}_j \dot{q}_k\right\} + \sum_{i=1}^{n} m_i g^T T_i^0 \begin{bmatrix} p_{ci} \\ 1 \end{bmatrix}$$

then, the Lagrange equation shows that the robot dynamics (3) can be expressed componentwise as

$$\sum_{k=1}^{n} m_{i,k}\ddot{q}_k + \sum_{k=1}^{n} c_{i,k}\dot{q}_k + g_i + f_i(\dot{q}_i) = \tau_i, \qquad i = 1, \ldots, n \tag{14}$$

where

$$m_{i,k} = \sum_{j=1}^{n} \text{trace}\left\{\frac{\partial T_{cj}^0}{\partial q_k} I_{cj} \left(\frac{\partial T_{cj}^0}{\partial q_i}\right)^T\right\} \tag{15}$$

$$c_{i,k} = \sum_{m=1}^{n}\left[\sum_{j=1}^{n} \text{trace}\left\{\frac{\partial^2 T_{cj}^0}{\partial q_k \partial q_m} I_{cj} \left(\frac{\partial T_{cj}^0}{\partial q_i}\right)^T\right\}\right]\dot{q}_m \tag{16}$$

$$g_i = -\sum_{j=1}^{n} m_j g^T \frac{\partial T_j^0}{\partial q_i} \begin{bmatrix} p_{cj} \\ 1 \end{bmatrix} \tag{17}$$

such that the entries of the coefficient matrices $M(q)$, $C(q, \dot{q})$ and $G(q)$ are given by m_{ik}, c_{ik}, and g_i respectively.
From Section 2.2.3 the entries of the term $F_s(\dot{q}) \in \mathbb{R}^n$, which models the static friction forces, are given by

$$f_{s,i}(\dot{q}_i) = B_{v,i}\dot{q}_i + B_{f1,i}\left(1 - \frac{2}{1 + e^{2w_{1,i}\dot{q}_i}}\right) + B_{f2,i}\left(1 - \frac{2}{1 + e^{2w_{2,i}\dot{q}_i}}\right) \tag{18}$$

The equations (14) - (18) have been implemented in Maple and applied to obtain the CFT-robot dynamics. The dynamic model of the CFT-robot is presented in Section 4.2.

2.2.5 Properties of the dynamic model

If the dynamic model (3), (4) has been obtained according to the Euler-Lagrange approach and the friction forces $\tau_f = F_s(\dot{q})$ are modelled according to (13), then it has the following properties, see [5], [10].

- The matrix $\dot{M}(q) - 2C(q, \dot{q})$ is skew symmetric, i.e.

$$x^T\left(\dot{M}(q) - 2C(q, \dot{q})\right)x = 0 \qquad \text{for all} \quad x \in \mathbb{R}^n \tag{19}$$

- In addition, $C(q,\dot{q})$ can be written as

$$C(q,\dot{q}) = \begin{bmatrix} \dot{q}^T C_1(q) \\ \vdots \\ \dot{q}^T C_n(q) \end{bmatrix} \tag{20}$$

where $C_j(q) \in \mathbb{R}^{n\times n}$ $j = 1,\ldots,n$ are symmetric matrices. It follows that for any scalar α and for all $q,x,y,z \in \mathbb{R}^n$

$$\begin{aligned} C(q,x)y &= C(q,y)x \\ C(q,z+\alpha x)y &= C(q,z)y + \alpha C(q,x)y \end{aligned} \tag{21}$$

- $M(q)$, $C(q,\dot{q})$ and $G(q)$ are bounded with respect to q

$$0 < M_m \leq \|M(q)\| \leq M_M \qquad \text{for all} \quad q \in \mathbb{R}^n \tag{22}$$

$$\|C(q,x)\| \leq C_M \|x\| \qquad \text{for all} \quad q,x \in \mathbb{R}^n \tag{23}$$

$$\|G(q)\| \leq g_b(q) \qquad \text{for all} \quad q \in \mathbb{R}^n \tag{24}$$

where $g_b(q)$ is a scalar function that can be determined for any robot. For a revolute arm $g_b(q)$ is constant and therefore independent of the joint vector q, but when prismatic joints are present, then $g_b(q)$ may depend on q.

- The friction forces represented by $F_s(\dot{q})$, with entries given by (18), are bounded with respect to $\dot{q}$

$$\|F(\dot{q})\| \leq b_v \|\dot{q}\| + b_{f1} + b_{f2} \qquad \text{for all} \quad \dot{q} \in \mathbb{R}^n \tag{25}$$

- The dynamic model (3) is linear in the parameters, and therefore it accepts a linear parametrization of the form

$$M(q,\theta_l)\ddot{q} + C(q,\dot{q},\theta_l)\dot{q} + G(q,\theta_l) = Y_r(q,\dot{q},\dot{q},\ddot{q})\theta_l \tag{26}$$

where θ_l is the parameter vector, and $Y_r(q,\dot{q},\dot{q},\ddot{q})$ denotes the regressor matrix, that contains nonlinear but known functions.

- The friction model (13) includes parameters, w_1 and w_2, that cannot be considered in the linear parametrization (26). Nonetheless the friction model can be parameterized as

$$F_s(\dot{q},\theta_f) = Y_f(\dot{q},\theta_f) \tag{27}$$

with θ_f a vector of parameters related to friction and $Y_f(\dot{q},\theta_f)$ a nonlinear regressor function.

- The parameterized models (26) and (27) can be combined into a general regressor for the total dynamic model of the robot as

$$M(q,\theta)\ddot{q} + C(q,\dot{q},\theta)\dot{q} + G(q,\theta) + F_s(\dot{q},\theta) = Y_r(q,\dot{q},\dot{q},\ddot{q})\theta + Y_f(\dot{q},\theta) \tag{28}$$

with $\theta = \begin{bmatrix} \theta_l & \theta_f \end{bmatrix} \in \mathbb{R}^p$.

2.3 Identification of physical parameters

As mentioned the physical parameters have to be identified or estimated since they cannot be measured or known a priori. There exist different estimation techniques which mainly differed in the computational effort when implemented.
There exist several techniques for identification of parameters, see for instance [6] and [11] for a general overview about identification theory . The most common classification of these techniques is based on the way they are applied: in closed loop or in open loop. Meanwhile based on the estimation routine the most popular techniques are Kalman filter, see [6], and linear least squares estimation, with its variants: recursive least squares estimation, linear least squares estimation and maximum likelihood estimation, see [4] and [12]. Most of the above mentioned techniques highly depend on the trajectories that are commanded to the system, such that conditions as persistence

of excitation and nonsingularity of the innovation terms are very common in identification theory. Nowadays, it has become common that the trajectories of the system for identification purposes are designed such that some optimization criterion is fulfilled, e.g. the approaches presented in [4] and [12]. As a result more reliable estimated parameters and larger bandwidth of the model plus the estimated parameters can be obtained.
According to Table 5, the CFT-robot presents a very limited span of motion in the Cartesian degrees of freedom, particularly x_{c1}, x_{c2} and x_{c4}. The limits in the CFT-robot makes open loop identification not suitable since the robot easily runs out of the Cartesian limits.
In the present report the Extended Kalman Filter is chosen to estimate the friction parameters. In particular the parameters $w_{1,i}$ and $w_{2,i}$ which appear in the exponential terms in (18) and thus cannot be considered in the linear parametrization (26). Once the friction parameters have been identified the linear least square method is used to identified the linear parameters by considering the linear parametrization (26).
From the assumption that the static friction effects are decoupled for each joint, see (12) it follows that each joint can be excited separately and those its friction parameters can be estimated independently. When exciting one of the joints of the robot, say joint i, and keeping the remanning in a fixed position (set point regulation), it follows that there is not Coriolis and centripetal forces in the dynamic model (3). Also the inertia matrix reduces to a scalar that is only function of the joint position q_i, i.e. from (3), (11) and (18) the dynamics for the i-th excited joint is given by

$$m(q_i)\ddot{q}_i + g(q_i) + B_{v,i}\dot{q}_i + B_{f1,i}\left(1 - \frac{2}{1+e^{2w_{1,i}\dot{q}_i}}\right) + B_{f2,i}\left(1 - \frac{2}{1+e^{2w_{2,i}\dot{q}_i}}\right) = \tau_i \tag{29}$$

Note that only the friction terms are function of the velocity $\dot{q}_i$. Ideally if the joint velocity $\dot{q}_i$ is kept constant the inertial dependency $m(q_i)\ddot{q}_i$ can be neglected, since for constant joint velocity $\dot{q}_i$ the joint acceleration is $\ddot{q}_i = 0$.
If the joints in the robot are excited one at a time, then by considering the dynamic model (29) the friction parameters can be estimated for each joint. Once the friction parameters are estimated, one can consider all the degrees of freedom of the robot and focus in estimating the linear physical parameters θ_l defined by the linear parametrization (26). To estimate the friction parameters the extended Kalman filter is considered.

2.3.1 Extended Kalman filter

The major advantage of the extended Kalman filter is that non-linear models in the parameters can be considered. For estimation of the physical parameters of a robot, particularly friction parameters which may appear as argument of non-linear functions, the extended Kalman filter is easy to implement and have good convergence properties.
In this report the continuous-discrete extended Kalman filter is considered, see [6]. A brief description of the method is as follows.
Consider the dynamic model of the i-th joint of a robot given by (29), with states $x_1 = q$ and $x_2 = \dot{q}$. Take the physical parameters in the model (29) as extra states. Then the extended dynamic model can be written as

$$\dot{x}(t) = f(x(t)) + W(t); \qquad W(t) \sim N(0, Q(t)) \tag{30}$$

$$y_k = h_k(x(t_k)) + V_k; \qquad V_k \sim N(0, R_k) \tag{31}$$

where $f(x(t))$ is a vector of nonlinear functions with zero rows which correspond to the extra states related to the physical parameters in (29). y_k is the measurement model which is discrete, and $W(t), V_k$ are zero mean Gaussian noises with spectral density matrix $Q(t)$ and R_k respectively. Throughout this report the instant of time t at the sampling k is denoted as t_k.
Assume that the noises $W(t), V_k$ are such that the expectation $E[W(t)V_k^T] = 0$ for all k and all t. Define the Jacobian matrices $F(\widehat{x}(t))$ and $H_k(\widehat{x}_k)$ as

$$F(\widehat{x}(t)) = \left.\frac{\partial f(x(t))}{\partial x(t)}\right|_{x(t)=\widehat{x}(t)} \tag{32}$$

$$H_k(\widehat{x}_k) = \left.\frac{\partial h_k(x(t_k))}{\partial x(t_k)}\right|_{x(t_k)=\widehat{x}_k} \tag{33}$$

where $\widehat{x}(t)$ is the continuous time state estimate and $\widehat{x}_k$ is the discrete time state estimate.
Then for the initial conditions $x(0) \sim N(\widehat{x}_0, P_0)$, where $\widehat{x}_0$ and P_0 are the initial conditions of the discrete estimated state $\widehat{x}_k$ and error covariance P_k, the continuous time propagation of the estimated state and error covariance are given by

$$\dot{\widehat{x}}(t) = f(\widehat{x}(t)) \tag{34}$$
$$\dot{P}(t) = F(\widehat{x}(t))P(t) + P(t)F(\widehat{x}(t))^T + Q(t) \tag{35}$$

while the discrete time state estimate and error covariance updating is given by

$$\widehat{x}_{k+1} = \widehat{x}_k + K_k[y_k - h_k(\widehat{x}_k)] \tag{36}$$
$$P_{k+1} = [I - K_k H_k(\widehat{x}_k)]P_k \tag{37}$$

with the gain matrix K_k given by

$$K_k = P_k H_k^T(\widehat{x}_k)\left[H_k(\widehat{x}_k)P_k H_k^T(\widehat{x}_k) + R_k\right]^{-1} \tag{38}$$

2.3.2 Linear least squares estimation

From the property of linearity in the parameters (26) it follows that the dynamic model of a robot (3) can be written as a parametric model given by

$$M(q,\theta_l)\ddot{q} + C\left(q,\dot{q},\theta_l\right)\dot{q} + G(q,\theta_l) = Y_\tau(q,\dot{q},\dot{q},\ddot{q})\theta_l \tag{39}$$

where θ_l is the vector of unknown parameters, and $Y(q,\dot{q},\dot{q},\ddot{q})$ denotes the regressor matrix, that contains nonlinear but known functions.
From the dynamic model (3) and the parametric model (39) it follows that the dynamics of the robot can be written as a minimal set of linear equations

$$Y_\tau(q,\dot{q},\dot{q},\ddot{q})\theta_l = \tau^\star \tag{40}$$

which relates measurements of the trajectories $q, \dot{q}, \ddot{q}$ and the non-conservative torque $\tau^\star$ to the set of parameters θ_l.
If it is assumed that the noise in all the measurements has the same standard deviation, then the standard linear least square estimation results in an estimated set of parameters given by

$$\hat{\theta}_l = F^+ b = (F^T F)^{-1} F^T b \tag{41}$$

where

$$F = \begin{bmatrix} Y_\tau(q(1),\dot{q}(1),\dot{q}(1),\ddot{q}(1)) \\ \vdots \\ Y_\tau(q(N),\dot{q}(N),\dot{q}(N),\ddot{q}(N)) \end{bmatrix}, \qquad b = \begin{bmatrix} \tau^\star(1) \\ \vdots \\ \tau^\star(N) \end{bmatrix} \tag{42}$$

with $q, \dot{q}, \dot{q}, \ddot{q}$ the collected data measurements, N the number of samplings.
The non conservative torques $\tau^\star$ for the linear least square estimation are given by (11), i.e. the measured external torque in the robot τ and the friction forces $F_s(\dot{q})$ obtained with the model (13) and the estimated friction parameters (obtained by the extended Kalman filter) and the measured data for $\dot{q}$.
The condition number of the matrix F is a measure for the sensitivity of the least squares solution $\hat{\theta}_l$ to perturbations on the elements of F and b provided that the matrix is well conditioned. The normalization of the matrix F, i.e. the division of its columns by their norm improves the condition number. Consequently it is better to estimate the model parameters using the normalized F matrix and scale the estimated model parameters afterwards.

2.3.3 Optimal robot excitation trajectories

The generation of optimal ("most exciting") excitation trajectories has been addressed in several papers, e.g. [4] and [12]. The main difference in several proposed approaches is the parametrization of the excitation trajectory. Most of the approaches in the literature involve nonlinear optimization

with motion constraints, such as constraints on joint positions, velocities and accelerations. In general the trajectory parametrization sets the degrees of freedom of the optimization problem such that the parameters allow to minimize or maximize a certain criterion.
One of the most common trajectory parametrization is to assume that the trajectory for each joint is a finite sum of sine and cosines functions, i.e. a finite Fourier series. Based on the approach presented in [12] it is assumed that the position q_i, velocity $\dot{q}_i$, and acceleration $\ddot{q}_i$ for the i-th joint of a $n-$degrees of freedom robot are given by

$$\begin{aligned} q_i(t) &= q_{i,0} + \sum_{l=1}^{N_i} \left[\frac{a_{i,l}}{l\omega_f} \sin(l\omega_f t) - \frac{b_{i,l}}{l\omega_f} \cos(l\omega_f t) \right] \\ \dot{q}_i(t) &= \sum_{l=1}^{N_i} [a_{i,l} \cos(l\omega_f t) + b_{i,l} \sin(l\omega_f t)] \\ \ddot{q}_i(t) &= \sum_{l=1}^{N_i} [-a_{i,l} l\omega_f \sin(l\omega_f t) + b_{i,l} l\omega_f \cos(l\omega_f t)] \end{aligned} \tag{43}$$

with ω_f the fundamental frequency of the Fourier series, such that these series have a period $T_f = 2\pi/\omega_f$. Each Fourier series contains $2N_i + 1$ parameters, that constitute the degrees of freedom for the optimization problem. Notice that $q_{i,0}$ is the offset on the position trajectory and may or may not be considered in the optimization problem depending of the specific robot.
The two most popular optimization criteria for designing excitation trajectories, among the various ones proposed in the literature, are the condition number J_k of the regression matrix F defined in (42) and the scalar measure $J_d = \log(\det(F^T F))$. The condition number J_k is a measure of the disturbance influence on the parameter estimates, meanwhile J_d represents the uncertainty of the parameter estimates. Note that both criteria depend on the joint positions, velocities and accelerations through the regressor matrix $Y_l(q, \dot{q}, \dot{q}, \ddot{q})$, but not on the model physical parameters θ_l.

3 CFT-robot: Cartesian space models

Denote the 4 Cartesian degrees of freedom of the CFT robot as x_{c1}, x_{c2}, x_{c3} and x_{c4}, such that x_{c1}, x_{c2} correspond to the up and down, forward and backward movement of the arm respectively, and x_{c3}, x_{c4} are the rotation and translation of the base in which the arm is mounted, see Figures 1 and 3.
Figure 3 shows a schematic diagram of the robot, x_{c3}, x_{c4} are absolute coordinates and are referred with respect to an inertial frame – frame $\{0\}$ – at the base of the robot. Meanwhile x_{c1}, x_{c2} are relative coordinates and are referred with respect to a frame at the edge of the translational platform – frame $\{e\}$. x_{c2} is defined under the consideration that the upper arm is aligned with the y_0 axis. x_{c4} is the distance from the origin of frame $\{0\}$ to the origin of frame $\{e\}$, i.e. the back edge of the translational base.
The origin of frame $\{0\}$ is located such that the x_0, y_0 axes define the plane of the base in which the rails are mounted, y_0 is aligned along the rails and crosses the middle point between the rails, and x_0 coincides with the Cartesian position $x_{c4} = 0$. The frame $\{0'\}$ defines the reference frame of the upper arm and its $x_{0'}$ axis coincides with the middle of the screw in which the reference for x_{c2} runs along. The frames $\{j\}$ for $j = 2, \ldots, 7$ are defined such that the origin coincides with the geometrical middle point of the link or structure they are attached to. The frame $\{1\}$ is located at the level of the rails in which the translational platform slides on. Moreover at least one of the axis of subsequent frames coincide or lie in the same plane. The offset in the definition of x_{c3} equal to 0.8292 [rad] is due to alignment of the encoder in the actuation motor; the offset value makes that the upper arm of the robot is aligned with the axis x_0 of the frame $\{0\}$ when $x_{c3} = 0.8292$.
The physical dimensions of the CFT-robot are listed in Table 1, where d_{i_i+1} denotes the distance between the origin of frame $\{i\}$ and $\{i+1\}$, d_s is the distance between the origins of frames $\{1\}$ and $\{e\}$, and L_i denotes the length of the $i-th$ link.
Consider the point P_e as the origin of frame $\{7\}$, then the coordinates of P_e with respect to the

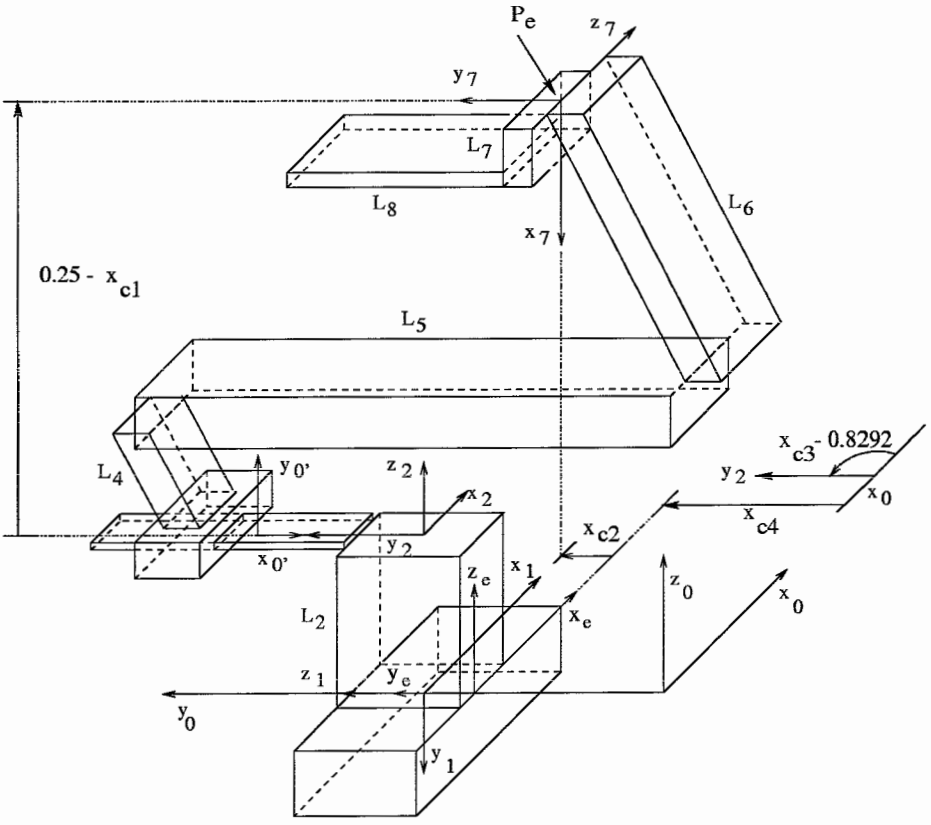

Figure 3: CFT-transposer: Cartesian coordinates

Dimension	Value $[m]$	Dimension	Value $[m]$
$L_2,\ d_{1\_2}$	0.25	L_8	0.48
L_4	0.05	$d_4,\ d_5$	0.00
L_5	0.35	d_6	0.04
L_6	0.30	d_s	0.185
L_7	0.08	$d_{2\_0'}$	0.0916

Table 1: Dimensions of the robot.

frame $\{0\}$ are given by

$$\begin{aligned} x_{P_e,0} &= (x_{c2} - d_s)\cos(x_{c3} - 0.8292) \\ y_{p_e,0} &= x_{c4} + d_s + (x_{c2} - d_s)\sin(x_{c3} - 0.8292) \\ z_{p_e,0} &= L_2 + 0.25 - x_{c1} \end{aligned} \tag{44}$$

Equations (44) determine any position of the point P_e in the robot working space as function of the robot Cartesian coordinates x_{c1}, x_{c2}, x_{c3} and x_{c4}.
The Cartesian coordinates x_{c3} and x_{c4} are directly actuated by the motors m_3 and m_4 respectively. But the upper arm is based on a pantograph design, such that x_{c1}, x_{c2} are indirectly moved by references that are set by the motors m_1 and m_2.

3.1 Kinematics of the upper arm

The vertical x_r and horizontal y_r reference values for the coordinates x_{c1}, x_{c2} are set by means of two slots which are actuated by the motors assigned as m_1 and m_2. Figure 4 shows a schematic diagram of the upper arm and the slots for the Cartesian reference variables x_r and y_r, i.e. from the origin of frame $\{0'\}$ to the point P_e. The relation between the reference values x_r, y_r and the Cartesian coordinates x_{c1}, x_{c2} is important because it establishes the correspondence between the Cartesian coordinates and the joint coordinates.

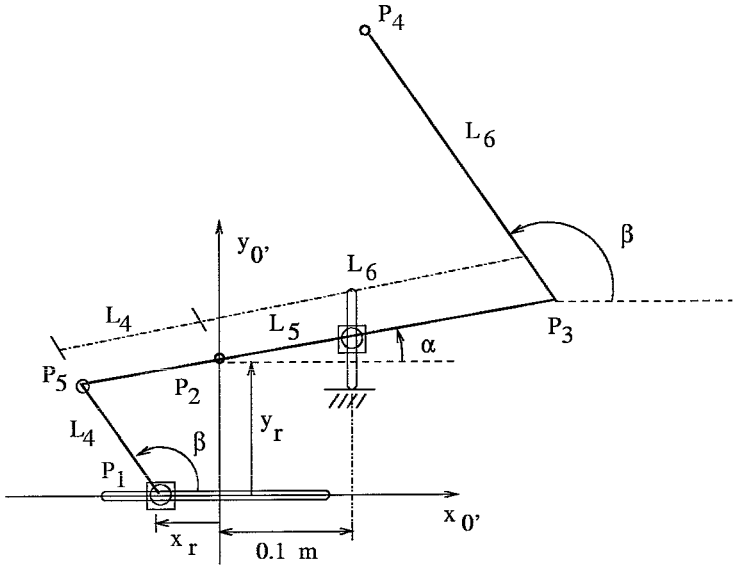

Figure 4: Upper arm: pantograph design.

The frame $\{0'\}$ defines the reference frame of the upper arm and its axis x'_0 coincides with the middle of the screw in which the horizontal reference variables x_r for x_{c2} runs along. The slots and frame $\{0'\}$ are fixed with respect to the frame $\{2\}$, see Figure 3.
In Figure 4, P_1, P_2 represent the points whose position is controlled by the servomotors through a ball-screw mechanism (spindle-nut). Both points slide along slots, such that P_1 sets the horizontal reference variable x_r and P_2 sets the vertical reference variable y_r. The angles α and β are relative to the horizontal axis and are defined counterclockwise. Notice that P_4 corresponds to point P_e of Figure 3 but with respect to the reference frame $\{0'\}$. Note that the length of link 5 holds that $L_5 = L_4 + L_6$.

Remark 2 *Because of the pantograph design there exist a physical constraint between the reference values x_r, y_r and the angles α, β. Therefore α, β are uniquely determine by x_r, y_r and vice versa. This constraint allows to define the correspondence between the Cartesian and the joint models.*

3.1.1 Relation between reference variables x_r, y_r and the coordinates x_{c1}, x_{c2}

The relevant coordinates to determine the kinematics are: (x_r, y_r), (α, β) and (x_4, y_4). However we need first to determine the coordinates of all the involved points

$$\begin{aligned} P_1 &= (x_r, 0) \\ P_2 &= (0, y_r) \\ P_3 &= (L_6 \cos(\alpha), y_r + L_6 \sin(\alpha)) \\ P_4 &= (L_6 (\cos(\alpha) + \cos(\beta)), y_r + L_6 (\sin(\alpha) + \sin(\beta))) \end{aligned} \tag{45}$$

the point P_5 can be expressed in two different ways

$$\begin{aligned} P_5 &= (x_r + L_4 \cos(\beta), L_4 \sin(\beta)) \\ P_5 &= (-L_4 \cos(\alpha), y_r - L_4 \sin(\alpha)) \end{aligned}$$

where L_4, L_5 and L_6 are the length of links 4, 5 and 6 respectively.
By equalizing the two expressions for point P_5 one obtains that

$$\begin{aligned} x_r &= -L_4 (\cos(\alpha) + \cos(\beta)) \\ y_r &= L_4 (\sin(\alpha) + \sin(\beta)) \end{aligned} \tag{46}$$

From the last equation of (45) and considering (46) it follows that

$$x_4 = -\frac{L_6}{L_4} x_r, \quad y_4 = \left(1 + \frac{L_6}{L_4}\right) y_r \tag{47}$$

The last equation determines a relation between the coordinates of the point P_4 and the reference variables (x_r, y_r). Note that the movements on point P_4 in x and y directions are decoupled. As a result movements on the reference variable x_r translates only in horizontal movements of point P_4, a similar situation occurs for the reference variable y_r and vertical movements of P_4.
From Figure 3 it follows that the coordinates of P_4 and the Cartesian coordinates x_{c1}, x_{c2}, with respect to frame $\{0'\}$, are related by

$$x_4 = d_{2\_0'} + d_s - x_{c2}, \quad y_4 = 0.25 - x_{c1}$$

and thus the relation between the reference variables x_r, y_r and the coordinates x_{c1}, x_{c2} is given by

$$x_r = \frac{L_4}{L_6}(x_{c2} - d_{2\_0'} - d_s) \tag{48}$$

$$y_r = \left(\frac{L_4}{L_4 + L_6}\right)(0.25 - x_{c1}) \tag{49}$$

Validation of the relation between (x_r, y_r) and (x_{c1}, x_{c2})

As a manner of validation and from the geometry of the robot, the relation between x_r, y_r and the coordinates x_{c1}, x_{c2}, given by (48, 49), can be determined via the span of the coordinates x_r, y_r and the span of the screws in which x_r, y_r slides.
From Table 5 in Appendix A it follows that x_{c2} has a span of 0.607 [m], meanwhile the screw in which x_r runs along has a span of 0.1012 [m], therefore between both spans there is a ratio of 6. On the other hand x_{c1}, y_r have a span of 0.315 [m] and 0.045 [m] respectively, and thus there is a ratio of 7 between them. Note that from Table 1 it follows that $\frac{L_6}{L_4} = 6$ and $\frac{L_4+L_6}{L_4} = 7$.
To determine the zero reference value for x_{c1} and x_{c2} and refer them to the zero reference on x_r, y_r, it is necessary to shift the variables x_{c1} and x_{c2} as function of their limits. Notice that the shifting in x_{c1} and x_{c2} must hold that the maximum displacements for x_{c1} and x_{c2} correspond to the maximum displacements on the screw for x_r, y_r. From Table 5 in Appendix A it follows that x_{c1} and x_{c2} must be shifted as $(x_{c2} + 0.0269)$ and $(0.0232 - x_{c1})$.
Note that in Figure 4 the axis $y_{0'}$ passes through the middle of the span of the screw in which x_r slides. Therefore there is a shift of 0.0506 m between the minimum position of the screw for x_r and the zero reference for x_r. Taking into account the ratio and shifts between x_{c2} and x_r it follows that they are related by

$$x_r = \frac{1}{6}(x_{c2} + 0.0269) - 0.0506 \tag{50}$$

which agrees with the relation given by (48) and the values in Table 1.
Also from Figure 4 notice that the screw in which y_r slides is not centered with respect to the axis $x_{0'}$, therefore there is a shift between the minimum position of the screw for y_r and the zero reference for y_r. From Figure 4 it follows that when $\alpha = 0$, $\beta = \pi/2$, the corresponding references are $x_r = -L_4$ and $y_r = L_4$. By setting this configuration in the robot, it has been determined that the nut in the screw for reference y_r was displaced 0.01765 [m] from its minimum position. Therefore there is a shift of 0.03235 [m] between the minimum position of the screw for y_r and the zero reference for y_r.Taking into account the ratio and shifts between x_{c1} and y_r it follows that

$$y_r = \frac{1}{7}(0.0232 - x_{c1}) + 0.03235 \tag{51}$$

which agrees with the relation given by (49) and the values in Table 1.

3.1.2 Relation between angular and translational variables α, β and x_r, y_r

Equations (48, 49) relate the Cartesian coordinates x_{c1}, x_{c2} with the reference variables y_r, x_r. But to relate the Cartesian coordinates to the joint coordinates it is necessary to determine the relation between y_r, x_r and the angles α, β.
Consider Figure 4 and focus on the triangle formed by P_1, P_2 and P_5. If the point P_1 is translated to the origin, then the coordinates of P_2 have changed to $(-x_r, y_r)$ and the distance from P_1 to P_2 is given by $r = \sqrt{x_r^2 + y_r^2}$, as it is depicted in Figure 5.

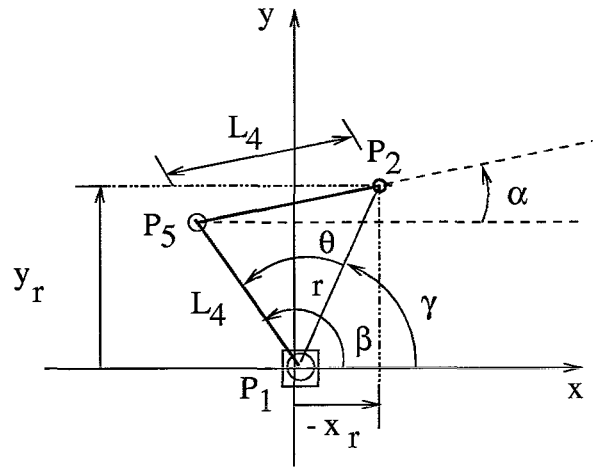

Figure 5: Relation between the variables α, β and x_r, y_r

On the one hand from Figure 5 and by considering standard trigonometric functions and the law of cosines it follows that

$$\begin{aligned} L_4^2 &= L_4^2 + r^2 - 2L_4 r\cos(\theta) \\ x_r &= -r\cos(\gamma) \end{aligned}$$

such that

$$\beta = \gamma + \theta = \arccos\left(\frac{-x_r}{r}\right) + \arccos\left(\frac{r}{2L_4}\right) \tag{52}$$

On the other hand from equations (46) and in order to have the proper sign of the angle it follows that

$$\alpha = \begin{cases} \arcsin\left(\frac{y_r}{L_4} - \sin(\beta)\right) & x_r < 0 \\ \arccos\left(\frac{-x_r}{L_4} - \cos(\beta)\right) & 0 \leq x_r \end{cases} \tag{53}$$

The relationships (52, 53) relate the angles α, β formed between the links at the upper arm with the horizontal and vertical reference variables x_r, y_r, which are displacements. The angles α, β can be used to define joint coordinates in the joint space of the robot.

4 CFT-robot: joint space models

In this section the approaches for kinematics and dynamics of a robot manipulator presented in Section 2.1 and 2.2 are applied to the CFT-robot. The kinematic model of the CFT-robot is presented in Section 4.1, and the dynamics in Section 4.2.
The relation between forces in the Cartesian space and torques in the joint space is presented in Section 4.3.

4.1 CFT robot kinematics

First the reference frames are assigned to the links and then the Denavit-Hartenberg parameters are obtained. Once the joint coordinates have been defined, through the Denavit-Hartenberg parameters, their relation to the Cartesian coordinates $x_{c1}, x_{c2}, x_{c3}, x_{c4}$ is established. Then the direct kinematics from the end effector position to a reduced set of joint variables is obtained.

4.1.1 Denavit-Hartenberg parameters

The coordinate frames are assigned as shown in Figure 6, the corresponding set of Denavit-Hartenberg parameters is listed in Table 2. L_i is the length of link i, d_i is the offset of each link along the z_i-axis, all the values are listed in Table 1. The joint coordinates q_1, q_3 are the

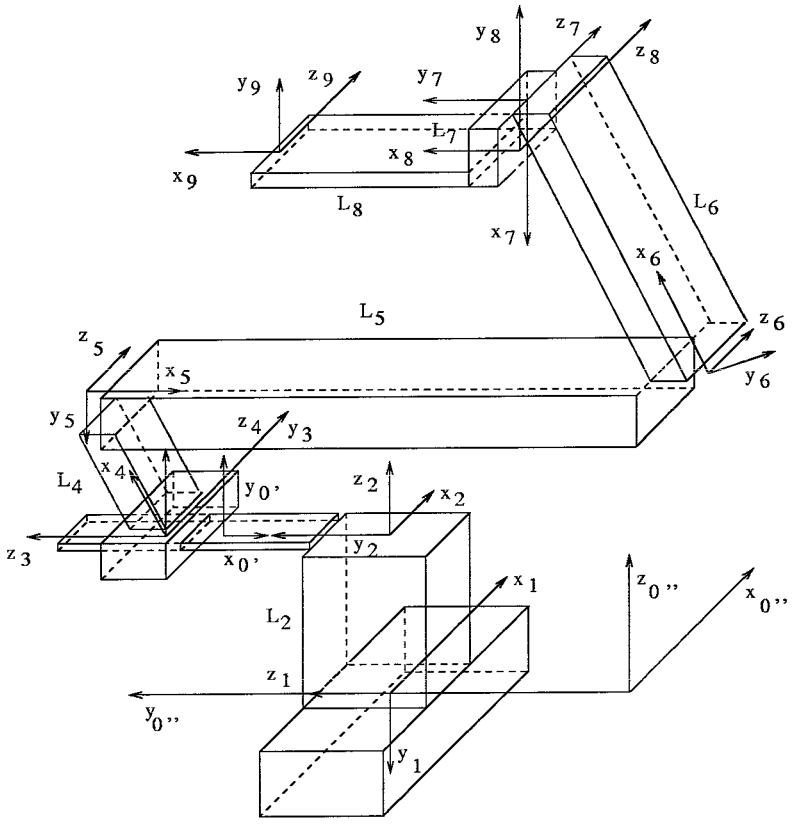

Figure 6: Frames for the CFT-transposer robot

translations along z_1, z_3 respectively. For $i = 2, 4, 5, 6, 7$ the joint coordinate q_i is the rotation angle about the z_i-axis.
By construction and the way how the frames $\{5\}, \{6\}$ and $\{7\}$ have been assigned, the link offsets d_6, d_7 are such that $d_7 = -d_6$, with $d_6 = 0.04$ [m].

Remark 3 *Because of the way the frames have been assigned in Figure 6, the rotational joint variables are defined clockwise. This fact has to be taken into account when the relation between Cartesian and joint coordinates is established, since the angles α and β in the Cartesian space, given by (53) and (52), are defined counterclockwise.*

4.1.2 Reduced set of joint coordinates

Table 2 accounts for 7 joint coordinates, including the rotation q_7 on the passively actuated tool. However, as mentioned in the introduction, the tool is kinematically constrained, such that it is

i	a_i	α_i	d_i	q_i
0	0	$-\frac{\pi}{2}$	—	—
1	0	$\frac{\pi}{2}$	q_1	0
2	0	$-\frac{\pi}{2}$	L_2	q_2
3	0	$-\frac{\pi}{2}$	q_3	$-\frac{\pi}{2}$
4	L_4	0	0	q_4
5	L_5	0	0	q_5
6	L_6	0	d_6	q_6
7	L_7	0	d_7	q_7
8	L_8	0	0	$\frac{\pi}{2}$
9	—	—	0	0

Table 2: Denavit-Hartenberg parameters for the CFT-robot

horizontal at all time. This constraint is satisfied if q_7 is such that

$$q_7 = \pi - q_4 \tag{54}$$

Furthermore, because of the pantograph design of the upper arm, see Figure 4, it follows that $q_6 = -q_5$. Therefore at this point the joint space of the CFT-robot can be reduced to 5 joint coordinates, i.e. $\{q_1, q_2, q_3, q_4, q_5\}$. However the Cartesian space has only 4 coordinates, $\{x_{c1}, x_{c2}, x_{c3}, x_{c4}\}$ and thus to be able to relate the Cartesian and the joint coordinates, one more joint coordinate has to be rewritten as function of the remaining ones.
From Figures 4, 6, and Remark 2 it follows that q_3, q_4, q_5 are uniquely determined by x_r, y_r – via the angles α, β, equations (53) and (52) – and vice versa, so any of the joint coordinates q_3, q_4, q_5 can be written as function of the other two. In order to work hereafter with only rotational joints in the upper arm, the translational joint coordinate q_3 is expressed as function of q_4, q_5 as follows. From Figures 4, 6 it follows that

$$\begin{aligned} q_3 &= -x_r + d_{2\_0'} \\ q_4 &= -\beta + \frac{\pi}{2} \\ q_5 &= \beta - \alpha \end{aligned} \tag{55}$$

therefore from (46) it follows that

$$q_3 = L_4 \left(\cos\left(-q_4 - q_5 + \frac{\pi}{2}\right) + \cos\left(-q_4 + \frac{\pi}{2}\right) \right) + d_{2\_0'} \tag{56}$$

Finally from equations (54), (56) and by considering $q_6 = -q_5$ the set of joint coordinates can be reduced to $\{q_1, q_2, q_4, q_5\}$. Moreover this reduced set of joint coordinates is related and uniquely determined by the Cartesian coordinates $\{x_{c1}, x_{c2}, x_{c3}, x_{c4}\}$, such that

$$\begin{aligned} q_1 &= x_{c4} + d_s \\ q_2 &= x_{c3} - 2.4 \\ q_4 &= -\beta + \frac{\pi}{2} \\ q_5 &= \beta - \alpha \end{aligned} \tag{57}$$

with $d_s = 0.185$, α, β given by (53) and (52) and the reference variables x_r, y_r given by (48, 49).

Remark 4 *Note that q_3 correspond to $-x_r$, therefore it is directly actuated by the motor m_2. On the other hand q_4, q_5 are indirectly actuated by the motors m_1, m_2. Thus, it can be considered that q_4, q_5 are actuated by virtual torques, that are determined by the Jacobian of the kinematic relation (46) and the forces generated by the motors m_1, m_2.*

4.1.3 End effector position of the CFT-robot

From Figure 6, the Denavit-Hartenberg parameters (Table 2), the homogeneous transformation (2), and the reduced set of joint coordinates $\{q_1, q_2, q_4, q_5\}$ the position and orientation of the end of the tool with respect to the base reference frame is given by

$$T_9^{0''} = T_1^{0''} T_2^1 T_3^2 T_4^3 T_5^4 T_6^5 T_7^6 T_8^7 T_9^8 \tag{58}$$

such that the position of the end of the tool, denoted by $p_T = [\ x_T \quad y_T \quad z_T\ ]^T$, is determined by the translational part of $T_9^{0''}$ as follows

$$\begin{aligned} x_T &= -(L_8 + d_{2\_0'}) \sin(q_2) + \frac{1}{2}\left[\cos(-q_2 + q_4) - \cos(q_2 + q_4)\right] L_6 + \\ &\quad + \frac{1}{2}\left[\cos(q_5 - q_2 + q_4) - \cos(q_5 + q_2 + q_4)\right](L_5 - L_4) \\ y_T &= q_1 + (L_8 + d_{2\_0'}) \cos(q_2) - \frac{1}{2}\left[\sin(q_2 + q_4) - \sin(-q_2 + q_4)\right] L_6 + \\ &\quad - \frac{1}{2}\left[\sin(q_5 - q_2 + q_4) + \sin(q_5 + q_2 + q_4)\right](L_5 - L_4) \\ z_T &= L_2 - L_7 + (L_6 + L_4) \cos(q_4) + L_5 \cos(q_4 + q_5) \end{aligned} \tag{59}$$

From Figures 3 and 6 it follows that the frames $\{0\}$ and $\{0''\}$ are equivalent. Therefore the position of the point P_e, given by (44), corresponds to the position given by (59) when $L_7 = 0$, $L_8 = 0$ is considered. Thus there exists a one to one relation from the joint kinematics (59) to the Cartesian kinematics (44).

4.2 CFT robot dynamics

The approach for modelling the dynamics of a robot, summarized by equations (15 - 18), has been implemented in Maple and applied to obtain the CFT-robot dynamics.
For simplicity the notation of the inertia matrix (8) has been changed to

$$I_{xxi} = \frac{-I^*_{xxi} + I^*_{yyi} + I^*_{zzi}}{2}, \qquad I_{yyi} = \frac{I^*_{xxi} - I^*_{yyi} + I^*_{zzi}}{2}, \qquad I_{zzi} = \frac{I^*_{xxi} + I^*_{yyi} - I^*_{zzi}}{2}$$

furthermore, the position vector p_{ci} of the center of gravity of link i in the frame $\{i\}$ is written as $p_{ci} = \begin{bmatrix} l_{xci} & l_{yci} & l_{zci} \end{bmatrix}^T$.
From Section 2.2 and the parameterized model (28) it follows that the dynamics of the CFT-robot can be written as

$$M(q,\theta)\ddot{q} + C(q,\dot{q},\theta)\dot{q} + G(q,\theta) + F(\dot{q},\theta) = \tau \tag{60}$$

where $\theta \in \mathbb{R}^p$ is a vector of physical parameters.
The reduced set of coordinates $\{q_1, q_2, q_4, q_5\}$ implies that the dynamic model of the CFT-robot is of $4th$ order, so $M(q,\theta)$, $C(q,\dot{q},\theta) \in \mathbb{R}^{4\times4}$, and $G(q,\theta), F(\dot{q},\theta) \in \mathbb{R}^{4\times1}$. After parametrization of the dynamics of the CFT robot it has been determined that the dynamic model for the CFT-robot has a minimum of 32 physical parameters. The set of parameters $\theta \in \mathbb{R}^{32}$ is given in Table 4, whit the estimated values obtained by the identification techniques presented in Section 2.3. The entries of the matrices $M(q,\theta)$, $C(q,\dot{q},\theta)$ and the vectors $G(q,\theta), F(\dot{q},\theta)$ are listed in Appendix B.

4.2.1 Parameters of the CFT-robot

The physical parameters θ_i, $i = 1,\ldots,32$ of the transposer robot have been estimated by the identification techniques presented in Section 2.3. First the parameters θ_i, $i = 13,\ldots,32$ related to the friction forces are estimated by using the extended Kalman filter. Then the remaining parameters θ_i, $i = 1,\ldots,12$ are identified by considering the linear least square method.
The least squares method (41) and the optimal excitation trajectories (43) are designed in the joint space, and as mentioned the optimization problem implies nonlinear motion constraints given by the joint limits in the robot.
For the CFT-robot the motion constraints determine the maximum and minimum limits of the Cartesian coordinates x_{c1}, x_{c2}, x_{c3} and x_{c4} (see Table 5). This limit motion constraints are hard to evaluate and may originate divergence of the optimization criterion given by the condition number J_k. The trajectories for identification purposes, denoted by $x_{ci,d}$, $i = 1,2,3,4$, are of the form given by (43). The Cartesian trajectories $x_{ci,d}$ are transformed by the relations (57) into joint trajectories $q_{j,d}$, $j = 1,2,4,5$, such that the functional J_k can be evaluated in the joint space.
The excitation trajectories in the Cartesian space $x_{ci,d}$, $i = 1,2,3,4$ of the form (43) are obtained by using the function FMINCON of the Optimization Toolbox of Matlab. It has been considered that the offset $x_{ci,0}$ $i = 1,2,3,4$ is equal to the middle point of the span of the Cartesian variable x_{ci}, see Table 5, i.e. $x_{c1,0} = -0.1343$ [m], $x_{c2,0} = 0.2766$ [m], $x_{c3,0} = 2.4$ [rad], and $x_{c4,0} = 0.0869$ [m].
The degrees of freedom on the optimization problem are the parameters $a_{i,l}$ and $b_{i,l}$, see equation (43). It has been considered that the trajectories $x_{ci,d}$, $i = 1,2,3,4$ have only 4 terms of each type, i.e. $N_i = 4$. The parameters of the optimal excitation trajectory of the form (43) are listed in Table 3. The corresponding condition number of the regression matrix is $J_k = 277.4$.
First the dynamic of the CFT-robot has been written in the form given by (60). The entries of the parameter vector $\theta \in \mathbb{R}^{32}$ are listed in Table 4. The value of the estimated parameters obtained by the extended Kalman filter and the least square estimation method are listed in Table 4.
The control τ for collecting the data to run the Kalman filter and the least square algorithm was set as a P-controller, with a desired trajectory $x_{ci,d}$, $i = 1,2,3,4$, given by the form (43) and

Parameter	$l=1$	$l=2$	$l=3$	$l=4$
$a_{1,l}$	-0.1102	0.0042	-0.0014	-0.0173
$a_{2,l}$	0.1629	-0.0118	0.1438	-0.0043
$a_{3,l}$	1.9698	0.0014	-0.0267	0.0021
$a_{4,l}$	0.0002	-0.0302	0.0021	-0.0800
$b_{1,l}$	0.0037	0.0009	0.0005	-0.0168
$b_{2,l}$	0.0188	-0.0257	0.0033	-0.0277
$b_{3,l}$	0.0011	0.0005	-0.0060	0.0024
$b_{4,l}$	-0.0347	0.0273	0.0294	0.0447

Table 3: Parameters of the excitation trajectories.

coefficients as in Table 3, with fundamental frequency of $\omega_f = 0.4$ Hz. The minimum ω_f and maximum $N_i\omega_f$ frequencies in (43) determine the bandwidth of the excitation trajectories.
The CFT robot is installed in the Dynamics and Control Technology Laboratory of the Department of Mechanical Engineering at the Eindhoven University of Technology. The robot for which the parameters have been identified has plate number 669358.
As a manner of validation of the dynamic model (60) and the estimated physical parameters listed in Table 4, a comparison study between measured τ and reconstructed (estimated) τ_e external torques is carried out. Figures 7 and 8 show the reconstructed $\tau_{e,j}$ (solid) and measured input control τ_j (dashed) for the joints $j = 1, 2, 4, 5$. The reconstructed input control $\tau_{e,j}$ is obtained from the dynamic model (60) and the estimated parameters listed in Table 4, by using the measured variables q_j, $\dot{q}_j$ and $\ddot{q}_j$ originated by the measured torque τ_j.

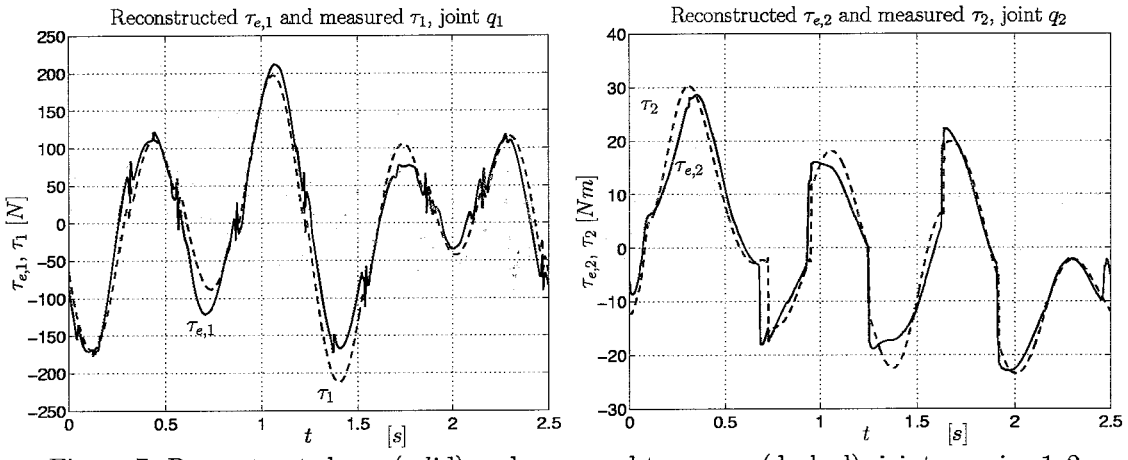

Figure 7: Reconstructed $\tau_{e,j}$ (solid) and measured torque τ_j (dashed), joints q_j, $j = 1, 2$.

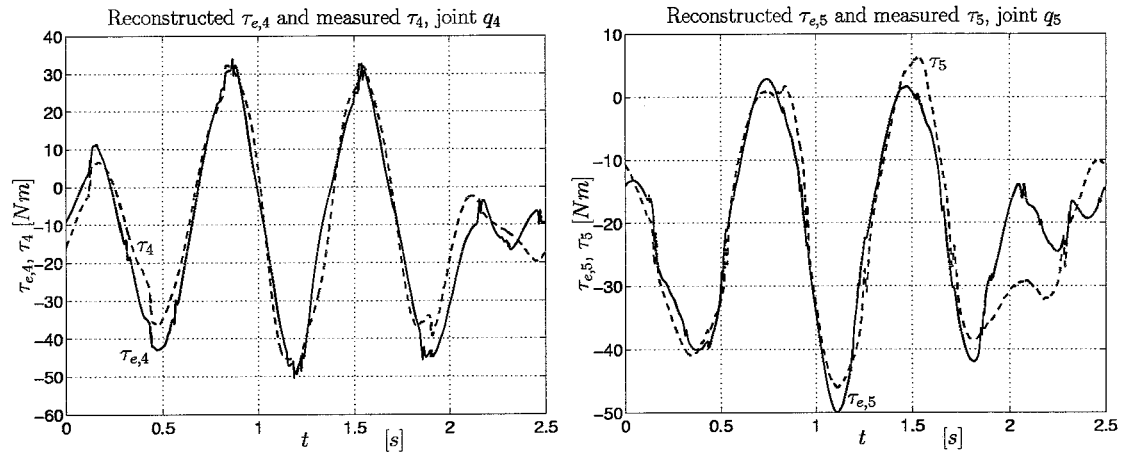

Figure 8: Reconstructed $\tau_{e,j}$ (solid) and measured torque τ_j (dashed), joints q_j, $j = 4, 5$.

Parameter	description	value
θ_1	$m_1 + m_2$	121.3049
θ_2	$m_2 l_{xc2}$	0.3107
θ_3	$m_2 l_{yc2}$	4.1955
θ_4	$m_2\left(l_{xc2}^2 + l_{yc2}^2\right) + m_3\left(l_{yc3}^2 + l_{zc3}^2\right) + m_4 l_{zc4}^2 + m_5 l_{zc5}^2 + m_6 l_{zc6}^2 + m_7\left(l_{yc7}^2 + l_{zc7}^2\right) + m_8\left(l_{xc8}^2 + l_{zc8}^2\right) + I_{xx2} + I_{yy2} + I_{yy3} + I_{zz3} + I_{zz4} + I_{zz5} + I_{zz6} + I_{yy7} + I_{zz7} + I_{xx8} + I_{zz8}$	1.7453
θ_5	$m_4 l_{xc4}$	0.8316
θ_6	$m_4 l_{yc4}$	0.8687
θ_7	$m_6 l_{xc6}$	0.8105
θ_8	$m_6 l_{yc6}$	1.6721
θ_9	$m_5 l_{xc5}$	-0.1879
θ_{10}	$m_5 l_{yc5}$	1.7850
θ_{11}	m_6	0.8759
θ_{12}	$m_7 + m_8$	4.1328
θ_{13}	B_{v1}	97.2600
θ_{14}	B_{v2}	9.0999
θ_{15}	B_{v4}	11.6257
θ_{16}	B_{v5}	9.6229
θ_{17}	$B_{f1,1}$	-54.9912
θ_{18}	$B_{f1,2}$	18.4710
θ_{19}	$B_{f1,4}$	-3.5232
θ_{20}	$B_{f1,5}$	-5.8564
θ_{21}	$B_{f2,1}$	-46.5915
θ_{22}	$B_{f2,2}$	11.1605
θ_{23}	$B_{f2,4}$	2.2684
θ_{24}	$B_{f2,5}$	8.2304
θ_{25}	$w_{1,1}$	150.3190
θ_{26}	$w_{1,2}$	136.8945
θ_{27}	$w_{1,4}$	-35.3699
θ_{28}	$w_{1,5}$	36.0641
θ_{29}	$w_{2,1}$	-98.9881
θ_{30}	$w_{2,2}$	-170.4702
θ_{31}	$w_{2,4}$	-89.3236
θ_{32}	$w_{2,5}$	16.2942

Table 4: Estimated parameters for the CFT transposer robot.

4.3 Force-Torque relations

Let τ denote the vector of joint external torques with the corresponding virtual joint displacements δq, and let δx represent the virtual Cartesian displacement caused by the force $\mathcal{F}$. Consider that the Cartesian and the joint coordinates are kinematically related by a function $x = h(q)$. Then the virtual displacements are related through the Jacobian $J(q) = \frac{dh(q)}{dq}$ according to

$$\delta x = J(q)\delta q$$

Base on the principle of virtual work, see [5] and [15], the work done in Cartesian space equals to the work done in joint space. So, from the definition of work we have that

$$\mathcal{F}^T \delta x = \tau^T \delta q$$

Therefore from the last two equations it follows that

$$\tau = J(q)^T \mathcal{F} \tag{61}$$

The last equation implies that the torque and force, which generate equivalent displacements in the robot, are related by the transpose of the Jacobian of the kinematic relation between the Cartesian and joint coordinates.
The relation (61) allows to convert any Cartesian quantity into a joint space quantity without calculating any inverse kinematic functions. For example, take any arbitrary robot with joint space dynamics defined by (3, 4) and let $x = h(q)$ denotes the kinematic relation between the end effector Cartesian position and the joint coordinates q, then the Cartesian space dynamics is given by

$$M_x(q)\ddot{x} + V_x(q,\dot{q}) + G_x(q) + F_x(\dot{q}, z) = \mathcal{F}$$

where

$$\begin{aligned} M_x(q) &= J^{-T}(q)M(q)J^{-1}(q) \\ V_x(q,\dot{q}) &= J^{-T}(q)\left(C(q,\dot{q})\dot{q} - M(q)J^{-1}(q)\dot{J}(q)\dot{q}\right) \\ G_x(q) &= J^{-T}(q)G(q) \\ F_x(\dot{q}, z) &= J^{-T}(q)\tau_f(\dot{q}, z) \end{aligned}$$

4.3.1 Forces and torques in the CFT robot

From (46) and the reduced set of joint coordinates $\{q_1, q_2, q_4, q_5\}$, given by (57), it follows that the actuated Cartesian coordinates and the joint coordinates are related by

$$\begin{aligned} x_{c4} &= q_1 - d_s \\ x_{c3} &= q_2 + 2.4 \\ x_r &= -L_4\left(\cos(-q_4 - q_5 + \frac{\pi}{2}) + \cos(-q_4 + \frac{\pi}{2})\right) \\ y_r &= L_4\left(\sin(-q_4 - q_5 + \frac{\pi}{2}) + \sin(-q_4 + \frac{\pi}{2})\right) \end{aligned}$$

which can be rewritten as

$$\begin{aligned} x_{c4} &= q_1 - d_s \\ x_{c3} &= q_2 + 2.4 \\ x_r &= -L_4\left(\sin(q_4 + q_5) + \sin(q_4)\right) \\ y_r &= L_4\left(\cos(q_4 + q_5) + \cos(q_4)\right) \end{aligned} \tag{62}$$

Denote the vector of Cartesian forces as $\mathcal{F}^T = [\ \mathcal{F}_{x_{c4}} \quad \mathcal{F}_{x_{c3}} \quad \mathcal{F}_{x_r} \quad \mathcal{F}_{y_r}\ ]$ and the vector of joint torques as $\tau^T = [\ \tau_{q_1} \quad \tau_{q_2} \quad \tau_{q_4} \quad \tau_{q_5}\ ]$, then from equation (61) and the kinematic relation (62) it follows that

$$\tau = \begin{bmatrix} \mathcal{F}_{x_{c4}} \\ \mathcal{F}_{x_{c3}} \\ -L_4\left(\mathcal{F}_{x_r}\left(\cos\left(q_4 + q_5\right) + \cos\left(q_4\right)\right) + \mathcal{F}_{y_r}\left(\sin\left(q_4 + q_5\right) + \sin\left(q_4\right)\right)\right) \\ -L_4\left(\mathcal{F}_{x_r}\cos\left(q_4 + q_5\right) + \mathcal{F}_{y_r}\sin\left(q_4 + q_5\right)\right) \end{bmatrix} \tag{63}$$

on the other hand the inverse relation is given by

$$\mathcal{F} = \begin{bmatrix} \tau_{q_1} \\ \tau_{q_2} \\ \frac{1}{\Delta_J}\left(-\tau_{q_4}\sin\left(q_4+q_5\right)+\tau_{q_5}\left(\sin\left(q_4+q_5\right)+\sin\left(q_4\right)\right)\right) \\ \frac{1}{\Delta_J}\left(\tau_{q_4}\cos\left(q_4+q_5\right)-\tau_{q_5}\left(\cos\left(q_4+q_5\right)+\cos\left(q_4\right)\right)\right) \end{bmatrix} \tag{64}$$

$$\Delta_J = L_4\left(\sin\left(q_4+q_5\right)\cos\left(q_4\right)-\cos\left(q_4+q_5\right)\sin\left(q_4\right)\right)$$

The relations (63) and (64) are based on the Jacobian of the kinematic relation (62), which relates the Cartesian reference variables x_r, y_r to the joint variables q_4, q_5, but not the Cartesian coordinates x_{c1}, x_{c2} explicitly. As mentioned x_{c1}, x_{c2} are not directly actuated by motors, so the voltage applied to the motors m_1, m_2 generate the forces that move x_r, y_r. Therefore those are the forces that have to be transformed into joint torques τ_{q_4}, τ_{q5}.
Notice that when a controller is implemented in the Cartesian space, it is based on the measurements x_{c1}, x_{c2}, however the measured voltages generate the forces $\mathcal{F}_{x_r}, \mathcal{F}_{y_r}$ in x_r, y_r. From equations (48, 49) it follows that there is a negative relation between x_{c1} and y_r, therefore there is a change of sign between the force generated by the controller and the force $\mathcal{F}_{y_r}$. Let $\mathcal{F}_{x_{c1}}$, $\mathcal{F}_{x_{c2}}$ denote the measured torques generated by a controller based on measurements x_{c1}, x_{c2}, then from (64) it follows that

$$\begin{bmatrix} \mathcal{F}_{x_{c4}} \\ \mathcal{F}_{x_{c3}} \\ \mathcal{F}_{x_{c2}} \\ \mathcal{F}_{x_{c1}} \end{bmatrix} = \begin{bmatrix} \tau_{q_1} \\ \tau_{q_2} \\ \frac{1}{\Delta_J}\left(-\tau_{q_4}\sin\left(q_4+q_5\right)+\tau_{q_5}\left(\sin\left(q_4+q_5\right)+\sin\left(q_4\right)\right)\right) \\ \frac{-1}{\Delta_J}\left(\tau_{q_4}\cos\left(q_4+q_5\right)-\tau_{q_5}\left(\cos\left(q_4+q_5\right)+\cos\left(q_4\right)\right)\right) \end{bmatrix} \tag{65}$$

and from (63)

$$\begin{bmatrix} \tau_{q_1} \\ \tau_{q_2} \\ \tau_{q_4} \\ \tau_{q_5} \end{bmatrix} = \begin{bmatrix} \mathcal{F}_{x_{c4}} \\ \mathcal{F}_{x_{c3}} \\ -L_4\left(\mathcal{F}_{x_{c2}}\left(\cos\left(q_4+q_5\right)+\cos\left(q_4\right)\right)-\mathcal{F}_{x_{c1}}\left(\sin\left(q_4+q_5\right)+\sin\left(q_4\right)\right)\right) \\ -L_4\left(\mathcal{F}_{x_{c2}}\cos\left(q_4+q_5\right)-\mathcal{F}_{x_{c1}}\sin\left(q_4+q_5\right)\right) \end{bmatrix} \tag{66}$$

The relations (65) and (66) transform effective external forces $\mathcal{F}_{x_{ci}}$ applied by the servomotors to external torques in the joint space τ_{q_j}, for $i = 1,2,3,4$, $j = 1,2,4,5$. Recall that the forces $\mathcal{F}_{x_{ci}}$ are proportional to the voltage applied at the servoamplifiers in the motors, with proportional gain given by K_T in Table 6.

5 Simulation model of the CFT-robot dynamics

As mentioned one of the purposes of developing mathematical models of a system, either kinematic or dynamic, is simulation.
The dynamic model of the CFT-robot given by the equation (60) with parameters θ listed in Table 4 has been implemented in Simulink. Figure 9 shows the block that simulates the CFT-robot dynamics in the Cartesian space. The inside of the block is shown in Figure 10.
The block in Figure 9 simulates the CFT-robot dynamics in the Cartesian space. The inputs in the block are the voltage in the servomotors corresponding to the Cartesian coordinates x_{ci}, for $i = 1, \ldots, 4$. The outputs of the block are the Cartesian coordinates x_{ci}, the status of the robot and the simulated time (which are included to obtain correspondence between the simulated robot dynamics and the real time robot interface), and the voltage applied in the servomotors (after the saturation that sets the limits in the servomotors).
Figure 10 shows the inside of the CFT-robot dynamics block in Figure 9. The block entitled "Direct Jacobian" corresponds to the Jacobian that transforms Cartesian forces in joint torques, (66), it includes the motor gains K_T listed in Table 6. The block entitled "Direct kinematics" correspond to the kinematic relation from the joint coordinates q_j to the Cartesian coordinates x_{ci} for $i = 1, \ldots, 4$ and $j = 1, 2, 4, 5$ given by (62) and the relation from x_r, y_r to x_{c1}, x_{c2} obtained from (48, 49). Notice that the Cartesian velocities $\dot{x}_{ci}$ are available in this block. However they are not considered as outputs to have correspondence to the real time robot interface.

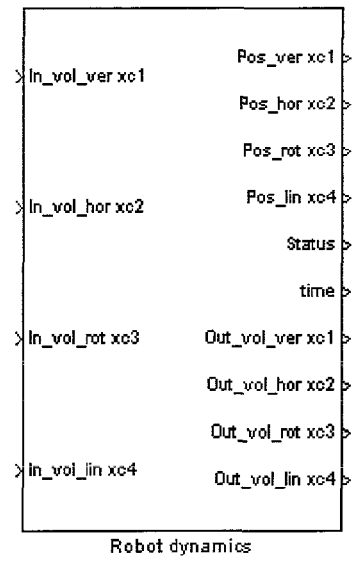

Figure 9: Block in Simulink: CFT-robot dynamics.

The block entitled "Lagrange model" correspond to the joint space dynamics of the CFT-robot given by (60). The function attached to this block has been programmed in C code as a S-function routine. The block has 8 parameters which correspond to the initial conditions in the Cartesian space $x_{ci}(0)$ and $\dot{x}_{ci}(0)$, for $i = 1, \ldots, 4$. Internally the initial conditions $x_{ci}(0)$ and $\dot{x}_{ci}(0)$ are transformed in initial conditions in the joint space $q_j(0)$ and $\dot{q}_j(0)$ by considering the kinematic relations given by (57).

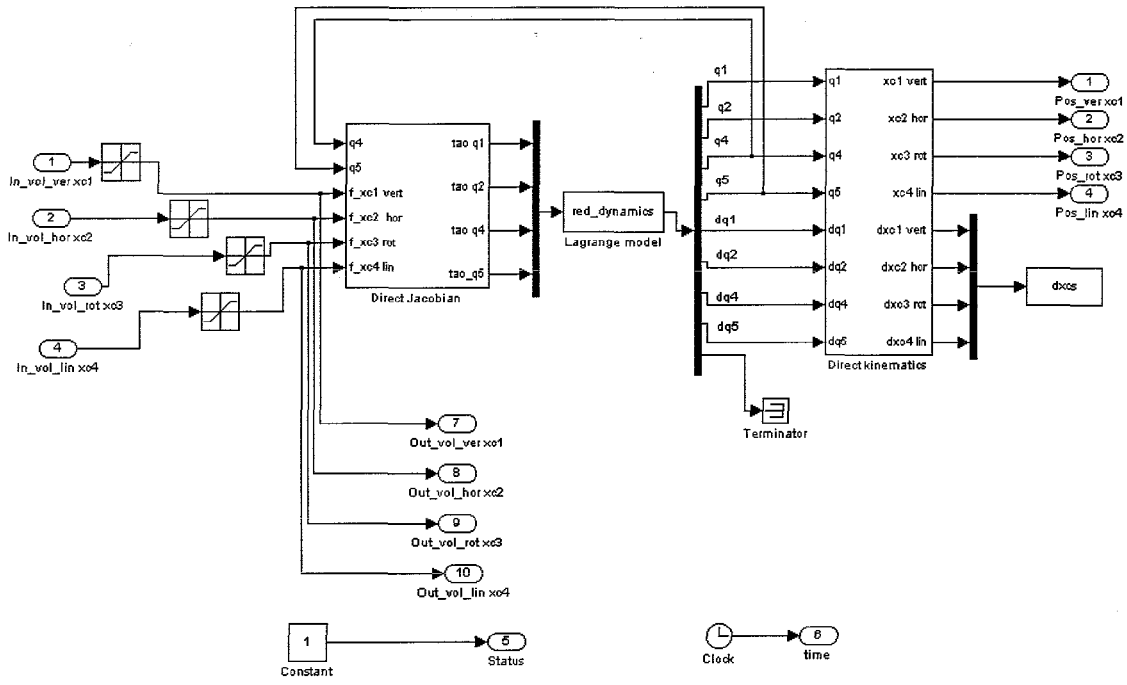

Figure 10: Inside of the block of the CFT-robot dynamics.

The files to simulate the dynamics of the CFT-robot can be found in the website http://www.wtb.tue.nl/ at the Dynamics and Control Group link.

Appendix A: Technical information of the CFT-robot

Some technical aspects of the CFT-robot which are relevant for modelling and identification are presented. The information is related to the encoder mounted on the shaft of the motors, the gear reduction ratios and torque gains. Most of this information has been obtained experimentally, and thus there is room for better measurements and calibration of the presented data.

A.1 Encoder measurements and limits of the robot

Each motor on the CFT robot is supplied with an encoder mounted in the rotor, the encoders have a resolution of 2000 PPR, see fabricator data sheet [14]. The scaling factors between the pulses of the encoders and their respective measurements are listed in Table 5, also the limits for each of the Cartesian coordinates are presented.

coordinate	encoder scaling factor	minimum limit	maximum limit
x_{c1}	8.7989×10^{-6}	-0.2918 [m]	0.0232 [m]
x_{c2}	7.5209×10^{-6}	-0.0269 [m]	0.5801 [m]
x_{c3}	1.6886×10^{-5}	-0.2892 [rad]	5.8708 [rad]
x_{c4}	5.0×10^{-6}	-0.0606 [m]	0.5344 [m]

Table 5: Encoder scaling factors and limits of the CFT-robot.

Remark 5 *At the Dynamics and Control Technology Laboratory there are two different setups working with CFT-robots. Although both setups use the same kind of robots there are some differences in the configuration. The values listed in Table 5 correspond to the setup working with TUeDACS. While for the setup working with dSPACE the limits in the Cartesian coordinate x_{c4} change to a minimum of -0.55 [m] and a maximum of 0.05 [m].*

A.2 Voltage-torque gains

The four Cartesian degrees of freedom are actuated by means of DC servomotors. The Cartesian coordinate x_{c4} and the references x_r, y_r are translational movements, such that there is a ratio between the torque applied by the motor and the force which originate x_{c4}, x_r, and y_r. All the motors are driven by servoamplifiers with a sensitivity of $K_a = 1.6$ [A/V] for the setup with TUeDACS and $K_a = 0.4$ [A/V] for the setup with dSPACE, see [13]. The motors have a torque constant, according to the fabrication sheet [14], of $K_t = 0.107$ [Nm/A], therefore the gain from the applied voltage in the servoamplifier to the torque in the motor is $K_V = 0.1712$ [Nm/V] for TUeDACS and $K_V = 0.0428$ [Nm/V] for dSPACE. Table 6 lists the gear ratios, conversion ratios and total gain from the voltage applied to the servoamplifiers to the force or torque in the respective coordinate.

Motor	Coordinate	Gear ratio K_g	Conversion ratio K_c	Total gain K_T TUeDACS	Total gain K_T dSPACE
m_1	y_r	$\frac{1}{2}$	$\frac{0.005}{2\pi}$ $\left[\frac{m}{rad}\right]$	430.2725 $\left[\frac{N}{V}\right]$	107.5681 $\left[\frac{N}{V}\right]$
m_2	x_r	$\frac{1}{2}$	$\frac{0.005}{2\pi}$ $\left[\frac{m}{rad}\right]$	430.2725 $\left[\frac{N}{V}\right]$	107.5681 $\left[\frac{N}{V}\right]$
m_3	x_{c3}	—	$\frac{6.16}{182\times 2\pi}$ $\left[\frac{rad}{rad}\right]$	31.7814 $\left[\frac{Nm}{V}\right]$	7.9453 $\left[\frac{Nm}{V}\right]$
m_4	x_{c4}	$\frac{1}{6}$	$\frac{0.06}{2\pi}$ $\left[\frac{m}{rad}\right]$	107.5681 $\left[\frac{N}{V}\right]$	26.8920 $\left[\frac{Nm}{V}\right]$

Table 6: Torque gains and conversion ratios.

The conversion ratio listed in Table 6 is considered after the gear reduction and relates the translation movement to the rotational movement of the respective coordinate. Although the gear ratios K_g and conversion ratios K_c have been determined by means of measurements on the robot, they agree with the values computed from the scaling factors and limits of the robot listed in Table 5.

The gear ratio for x_{c3} could not be determine by measurements because of the architecture of the robot. The conversion ratio for x_{c3} was determined by considering the scaling factor and the total span of the coordinate x_{c3} (see Table 5). The span of x_{c3} is 6.16 [rad], such that from the scaling factor and the resolution of the encoder it follows that the span of x_{c3} implies 182 revolutions of the rotor in motor m_3.

Appendix B: Dynamic model and estimated parameters of the CFT-robot

Here the entries of the dynamic model of the CFT transposer robot are presented.
The dynamics of the CFT transposer robots is given by (60), i.e.

$$M(q,\theta)\ddot{q} + C\left(q,\dot{q},\theta\right)\dot{q} + G(q,\theta) + F(\dot{q},\theta) = \tau \tag{67}$$

$$F(\dot{q},\theta) = B_v\dot{q} + B_{f1}\left(1 - \frac{2}{1+e^{2w_1\dot{q}}}\right) + B_{f2}\left(1 - \frac{2}{1+e^{2w_2\dot{q}}}\right) \tag{68}$$

Entries of the inertia matrix $M(q,\theta)$

The entries of the symmetric inertia matrix $M(q,\theta) \in \mathbb{R}^{4\times4}$, as function of the generalized joint coordinates $q = [\ q_1 \quad q_2 \quad q_4 \quad q_5\ ]^T$ and the parameters θ_j, $j = 1,\ldots 32$, listed in table 4, are given by

$$M_{1,1} = \theta_1 + \theta_{11} + \theta_{12}$$

$$\begin{aligned}
M_{1,2} &= (-\theta_{12}d_{2_0'} - \theta_{11}d_{2_0'} - \theta_3)\sin(q_2) + (\theta_2 + d_6\theta_{11})\cos(q_2) \\
&+\frac{1}{2}((L_4 - L_5)(\theta_{12} + \theta_{11}) - \theta_9)(\cos(q_5 + q_2 + q_4) - \cos(q_5 - q_2 + q_4)) \\
&+\frac{1}{2}(\theta_7 + \theta_5 + \theta_{12}L_6)(\cos(-q_2 + q_4) - \cos(q_2 + q_4)) \\
&+\frac{1}{2}(\theta_8 + \theta_6)(\sin(q_2 + q_4) - \sin(-q_2 + q_4)) \\
&+\frac{1}{2}(-\sin(q_5 - q_2 + q_4) + \sin(q_5 + q_2 + q_4))\theta_{10}
\end{aligned}$$

$$\begin{aligned}
M_{1,3} &= \frac{1}{2}(-\theta_5 - \theta_7 - \theta_{12}L_6)(\cos(q_2 + q_4) + \cos(-q_2 + q_4)) \\
&+\frac{1}{2}((L_4 - L_5)(\theta_{12} + \theta_{11}) - \theta_9)(\cos(q_5 - q_2 + q_4) + \cos(q_5 + q_2 + q_4)) \\
&+\frac{1}{2}(\theta_8 + \theta_6)(\sin(q_2 + q_4) + \sin(-q_2 + q_4)) \\
&+\frac{1}{2}(\sin(q_5 + q_2 + q_4) + \sin(q_5 - q_2 + q_4))\theta_{10}
\end{aligned}$$

$$\begin{aligned}
M_{1,4} &= \frac{1}{2}((L_4 - L_5)(\theta_{11} + \theta_{12}) - \theta_9)(\cos(q_5 + q_2 + q_4) + \cos(q_5 - q_2 + q_4)) \\
&+\frac{1}{2}(\sin(q_5 + q_2 + q_4) + \sin(q_5 - q_2 + q_4))\theta_{10}
\end{aligned}$$

$$
\begin{aligned}
M_{2,2} &= ((L_5 - L_4)(\sin(q_5) + \sin(q_5 + 2q_4)) - 2\cos(q_4)d_{2\_0'})\theta_8 + \theta_4 \\
&+(-2d_{2\_0'}\cos(q_4 + q_5) - L_4\sin(2q_5 + 2q_4))\theta_{10} + \theta_{12}d_{2\_0'}^2 \\
&+((\frac{1}{2} - \frac{1}{2}\cos(2q_5 + 2q_4))(L_5^2 + L_4^2) + 2L_4d_{2\_0'}\sin(q_4 + q_5) + d_6^2 \\
&+d_{2\_0'}^2 + ((\cos(2q_5 + 2q_4) - 1)L_4 - 2d_{2\_0'}\sin(q_4 + q_5))L_5)\theta_{11} \\
&+((\cos(2q_4) - \cos(q_5) - 1 + \cos(q_5 + 2q_4))L_4 \\
&-2d_{2\_0'}\sin(q_4))\theta_5 - 2(\sin(q_4 + q_5)L_5 + \sin(q_4)L_6)d_{2\_0'}\theta_{12} \\
&+((\cos(q_5 + 2q_4) - \cos(q_5))(L_4 - L_5) - 2d_{2\_0'}\sin(q_4))\theta_7 \\
&-\frac{1}{2}\theta_{12}(\cos(2q_4) - 1)L_6^2 - \frac{1}{2}(\cos(2q_5 + 2q_4) - 1)(L_5^2 + L_4^2)\theta_{12} \\
&+(-L_4(\sin(2q_4) + \sin(q_5 + 2q_4) + \sin(q_5)) - 2\cos(q_4)d_{2\_0'})\theta_6 \\
&+((\cos(2q_5 + 2q_4) - 1)L_4 + (\cos(q_5) - \cos(q_5 + 2q_4))L_6)L_5\theta_{12} \\
&+((\cos(2q_5 + 2q_4) - 1)L_4 - 2d_{2\_0'}\sin(q_4 + q_5))\theta_9 \\
&+(2\sin(q_4 + q_5)d_{2\_0'} - (\cos(q_5) + \cos(q_5 + 2q_4))L_6)L_4\theta_{12}
\end{aligned}
$$

$$
M_{2,3} = -\theta_7 d_6\cos(q_4) + \theta_8 d_6\sin(q_4) + \theta_{11}d_6(L_4 - L_5)\cos(q_4 + q_5)
$$

$$
M_{2,4} = \theta_{11}d_6(L_4 - L_5)\cos(q_4 + q_5)
$$

$$
\begin{aligned}
M_{3,3} &= (((L_5 - L_6)L_4 + 2L_5L_6)\theta_{12} + L_5L_4\theta_{11} + (\theta_9 - \theta_5 - \theta_7)L_4 \\
&+2\theta_7L_5)\cos(q_5) + L_4(\theta_6 + \theta_8)\sin(2q_4) \\
&-L_4((\frac{1}{2}L_4 + L_6)\theta_{12} + \frac{1}{2}L_4\theta_{11} + \theta_5 + \theta_7)\cos(2q_4) \\
&-L_4((L_6 + L_5)\theta_{12} + L_5\theta_{11} + \theta_9 + \theta_7 + \theta_5)\cos(q_5 + 2q_4) \\
&+(\theta_8 + \theta_{10} + \theta_6)L_4\sin(q_5 + 2q_4) + ((2L_5 - L_4)\theta_8 \\
&-(\theta_6 + \theta_{10})L_4)\sin(q_5) + (L_4^2 + (L_6 - L_5)L_4 + L_5^2 + L_6^2)\theta_{12} \\
&+((\frac{1}{2}L_4 - L_5)(\theta_{12} + \theta_{11}) - \theta_9)L_4\cos(2q_5 + 2q_4) \\
&+(L_5^2 - L_5L_4 + L_4^2)\theta_{11} + (\theta_7 - \theta_9 + \sin(2q_5 + 2q_4)\theta_{10} - \theta_5)L_4
\end{aligned}
$$

$$
\begin{aligned}
M_{3,4} &= \frac{1}{2}(\sin(q_5 + 2q_4) - \sin(q_5))L_4\theta_6 + \frac{1}{2}\theta_{12}(\cos(2q_5 + 2q_4) + 1)L_4^2 \\
&+(\frac{1}{2}\cos(q_5) - \cos(2q_5 + 2q_4) - \frac{1}{2}\cos(q_5 + 2q_4) - 1)L_4\theta_9 \\
&+(\frac{1}{2}\sin(q_5 + 2q_4) + \sin(2q_5 + 2q_4) - \frac{1}{2}\sin(q_5))L_4\theta_{10} \\
&+(L_5\cos(q_5) - \frac{1}{2}(\cos(q_5) + \cos(q_5 + 2q_4))L_4)\theta_7 \\
&+((L_5 - \frac{1}{2}L_4)\sin(q_5) + \frac{1}{2}L_4\sin(q_5 + 2q_4))\theta_8 + \theta_{12}L_5^2 \\
&+(L_5^2 + \frac{1}{2}(\cos(q_5) - \cos(q_5 + 2q_4))L_4L_5 + \frac{1}{2}(1 + \cos(2q_5 + 2q_4)) \\
&\times (L_4^2 - 2L_4L_5))\theta_{11} - \frac{1}{2}(\cos(q_5) + \cos(q_5 + 2q_4))L_4\theta_5 \\
&+(\cos(q_5)L_6 - \frac{1}{2}(2 + 2\cos(2q_5 + 2q_4) + \cos(q_5 + 2q_4) \\
&-\cos(q_5))L_4)L_5\theta_{12} - \frac{1}{2}\theta_{12}(\cos(q_5) + \cos(q_5 + 2q_4))L_6L_4
\end{aligned}
$$

$$
\begin{aligned}
M_{4,4} &= ((\frac{1}{2}L_4^2 - L_5L_4)(\theta_{12} + \theta_{11}) - L_4\theta_9)\cos(2q_5 + 2q_4) \\
&+(\frac{1}{2}L_4^2 - L_5L_4 + L_5^2)(\theta_{12} + \theta_{11}) + (\sin(2q_5 + 2q_4)\theta_{10} - \theta_9)L_4
\end{aligned}
$$

Entries of the Coriolis matrix $C(q,\dot{q},\theta)$

The entries of the Coriolis matrix $C(q,\dot{q},\theta) \in \mathbb{R}^{4\times 4}$, as function of the generalized joint coordinates $q = [\ q_1 \quad q_2 \quad q_4 \quad q_5\ ]^T$ and the parameters θ_j, $j = 1,\ldots 32$, listed in table 4, are given by

$$C_{1,1} = C_{2,1} = C_{3,1} = C_{4,1} = 0$$

$$\begin{aligned}
C_{1,2} &= \frac{1}{2}(\theta_7+\theta_5+L_6\theta_{12})((\dot{q}_2-\dot{q}_4)\sin(q_4-q_2)+(\dot{q}_2+\dot{q}_4)\\
&\times\sin(q_2+q_4))-((\theta_{12}+\theta_{11})d_{2_0'}+\theta_3)\dot{q}_2\cos(q_2)\\
&+\frac{1}{2}(\theta_9+(L_5-L_4)(\theta_{12}+\theta_{11}))((\dot{q}_4+\dot{q}_2+\dot{q}_5)\\
&\times\sin(q_5+q_2+q_4)+(\dot{q}_2-\dot{q}_4-\dot{q}_5)\sin(q_5-q_2+q_4))\\
&-(\theta_2+d_6\theta_{11})\dot{q}_2\sin(q_2)+\frac{1}{2}(\theta_8+\theta_6)((\dot{q}_2-\dot{q}_4)\cos(q_4-q_2)\\
&+(\dot{q}_2+\dot{q}_4)\cos(q_2+q_4))+\frac{1}{2}((\dot{q}_2-\dot{q}_4-\dot{q}_5)\\
&\times\cos(q_5-q_2+q_4)+(\dot{q}_4+\dot{q}_2+\dot{q}_5)\cos(q_5+q_2+q_4))\theta_{10}
\end{aligned}$$

$$\begin{aligned}
C_{1,3} &= \frac{1}{2}(\theta_8+\theta_6)((\dot{q}_4-\dot{q}_2)\cos(q_4-q_2)+(\dot{q}_2+\dot{q}_4)\cos(q_2+q_4))\\
&+\frac{1}{2}(\theta_9+(L_5-L_4)(\theta_{12}+\theta_{11}))((\dot{q}_4+\dot{q}_2+\dot{q}_5)\\
&\times\sin(q_5+q_2+q_4)+(\dot{q}_4-\dot{q}_2+\dot{q}_5)\sin(q_5-q_2+q_4))\\
&+\frac{1}{2}(\theta_5+\theta_7+L_6\theta_{12})((\dot{q}_4-\dot{q}_2)\sin(q_4-q_2)+(\dot{q}_2+\dot{q}_4)\\
&\times\sin(q_2+q_4))+\frac{1}{2}((\dot{q}_4+\dot{q}_2+\dot{q}_5)\cos(q_5+q_2+q_4)\\
&+(\dot{q}_4+\dot{q}_5-\dot{q}_2)\cos(q_5-q_2+q_4))\theta_{10}
\end{aligned}$$

$$\begin{aligned}
C_{1,4} &= \frac{1}{2}((\dot{q}_4+\dot{q}_2+\dot{q}_5)\cos(q_5+q_2+q_4)+(\dot{q}_4-\dot{q}_2+\dot{q}_5)\\
&\times\cos(q_5-q_2+q_4))\theta_{10}+\frac{1}{2}(\theta_9+(L_5-L_4)(\theta_{12}+\theta_{11}))\\
&\times((\dot{q}_4+\dot{q}_2+\dot{q}_5)\sin(q_5+q_2+q_4)\\
&+(\dot{q}_4+\dot{q}_5-\dot{q}_2)\sin(q_5-q_2+q_4))
\end{aligned}$$

$$\begin{aligned}
C_{2,2} &= -\frac{1}{2}(L_4\theta_6-L_5\theta_8+\theta_8L_4)((2\dot{q}_4+\dot{q}_5)\cos(2q_4+q_5)\\
&+\dot{q}_5\cos(q_5))-\dot{q}_4d_{2_0'}(\theta_5+\theta_7+L_6\theta_{12})\cos(q_4)\\
&-(\dot{q}_4+\dot{q}_5)(\theta_9+(L_5-L_4)(\theta_{12}+\theta_{11}))d_{2_0'}\cos(q_4+q_5)\\
&-\frac{1}{2}(\dot{q}_4+\dot{q}_5)(2L_4\theta_9-(L_5-L_4)^2(\theta_{12}+\theta_{11}))\sin(2q_5+2q_4)\\
&-\frac{1}{2}\dot{q}_4(2L_4\theta_5-L_6^2\theta_{12})\sin(2q_4)-\dot{q}_4L_4\theta_6\cos(2q_4)\\
&+\frac{1}{2}(L_4(\theta_5+\theta_7)+L_6\theta_{12}(L_4-L_5)-L_5\theta_7)(\dot{q}_5\sin(q_5)\\
&-(2\dot{q}_4+\dot{q}_5)\sin(2q_4+q_5))+(\dot{q}_4+\dot{q}_5)\sin(q_4+q_5)d_{2_0'}\theta_{10}\\
&-(\dot{q}_4+\dot{q}_5)\cos(2q_5+2q_4)L_4\theta_{10}+d_{2_0'}\dot{q}_4(\theta_8+\theta_6)\sin(q_4)
\end{aligned}$$

$$
\begin{aligned}
C_{2,3} &= \frac{1}{2}\dot{q}_2(L_6^2\theta_{12} - 2L_4\theta_5)\sin(2q_4) - \dot{q}_2\cos(2q_5+2q_4)L_4\theta_{10} \\
&+\frac{1}{2}\dot{q}_2((L_5-L_4)^2(\theta_{12}+\theta_{11}) - 2L_4\theta_9)\sin(2q_5+2q_4) \\
&+(\dot{q}_2 d_{2\_0'}\theta_{10} + d_6\theta_{11}(\dot{q}_4+\dot{q}_5)(L_5-L_4))\sin(q_4+q_5) \\
&-(((L_5-L_4)(\theta_{12}+\theta_{11})+\theta_9)d_{2\_0'})\dot{q}_2\cos(q_4+q_5) \\
&+\dot{q}_2((L_5-L_4)(L_6\theta_{12}+\theta_7) - L_4\theta_5)\sin(2q_4+q_5) \\
&+(\dot{q}_4 d_6\theta_8 - \dot{q}_2(L_6\theta_{12}+\theta_7+\theta_5)d_{2\_0'})\cos(q_4) \\
&+(\dot{q}_2(\theta_8+\theta_6)d_{2\_0'} + \dot{q}_4 d_6\theta_7)\sin(q_4) \\
&+\dot{q}_2((L_5-L_4)\theta_8 - L_4\theta_6)\cos(2q_4+q_5) - \dot{q}_2 L_4\theta_6\cos(2q_4)
\end{aligned}
$$

$$
\begin{aligned}
C_{2,4} &= ((\dot{q}_4+\dot{q}_5)(L_5-L_4)d_6\theta_{11} + \dot{q}_2 d_{2\_0'}\theta_{10})\sin(q_4+q_5) \\
&+\frac{1}{2}\dot{q}_2((L_5-L_4)^2(\theta_{12}+\theta_{11}) - 2L_4\theta_9)\sin(2q_5+2q_4) \\
&-((L_5-L_4)(\theta_{12}+\theta_{11})+\theta_9)d_{2\_0'}\dot{q}_2\cos(q_4+q_5) \\
&-\dot{q}_2 L_4\theta_{10}\cos(2q_5+2q_4) \\
&-\frac{1}{2}\dot{q}_2(L_4\theta_6 + \theta_8(L_4-L_5))(\cos(q_5)+\cos(2q_4+q_5)) \\
&+\frac{1}{2}\dot{q}_2((L_5-L_4)(L_6\theta_{12}+\theta_7) - L_4\theta_5)(\sin(2q_4+q_5)-\sin(q_5))
\end{aligned}
$$

$$
\begin{aligned}
C_{3,2} &= \dot{q}_2 L_4\theta_{10}\cos(2q_5+2q_4) + \dot{q}_2 L_4\theta_6\cos(2q_4) \\
&+\dot{q}_2 d_{2\_0'}(\theta_9 + (L_5-L_4)(\theta_{12}+\theta_{11}))\cos(q_4+q_5) \\
&-\dot{q}_2 d_{2\_0'}\sin(q_4+q_5)\theta_{10} + \frac{1}{2}\dot{q}_2(2L_4\theta_5 - L_6^2\theta_{12})\sin(2q_4) \\
&+\dot{q}_2(L_4\theta_5 - (L_5-L_4)(L_6\theta_{12}+\theta_7))\sin(2q_4+q_5) \\
&+\frac{1}{2}\dot{q}_2(-(L_5-L_4)^2(\theta_{12}+\theta_{11}) + 2L_4\theta_9)\sin(2q_5+2q_4) \\
&+\dot{q}_2 d_{2\_0'}(\theta_5+\theta_7+L_6\theta_{12})\cos(q_4) - \dot{q}_2 d_{2\_0'}(\theta_8+\theta_6)\sin(q_4) \\
&+\dot{q}_2(L_4\theta_6 + \theta_8(L_4-L_5))\cos(2q_4+q_5)
\end{aligned}
$$

$$
\begin{aligned}
C_{3,3} &= \frac{1}{2}L_4(\dot{q}_4+\dot{q}_5)\left((2L_5-L_4)(\theta_{12}+\theta_{11}) + 2\theta_9\right)\sin(2q_5+2q_4) \\
&-\frac{1}{2}\dot{q}_5((2L_5L_6 - L_6L_4 + L_5L_4)\theta_{12} + (2L_5-L_4)\theta_7 + \theta_{11}L_5L_4 \\
&+L_4(\theta_9-\theta_5))\sin(q_5) + L_4(\dot{q}_4+\dot{q}_5)\theta_{10}\cos(2q_5+2q_4) \\
&+\frac{1}{2}L_4(2\dot{q}_4+\dot{q}_5)((L_5+L_6)\theta_{12} + \theta_7 + L_5\theta_{11} + \theta_5 + \theta_9) \\
&\times\sin(2q_4+q_5) + L_4\dot{q}_4(\theta_8+\theta_6)\cos(2q_4) \\
&+\frac{1}{2}L_4\dot{q}_4((L_4+2L_6)\theta_{12} + 2\theta_7 + L_4\theta_{11} + 2\theta_5)\sin(2q_4) \\
&+\frac{1}{2}L_4(2\dot{q}_4+\dot{q}_5)(\theta_8+\theta_6+\theta_{10})\cos(2q_4+q_5) \\
&-\frac{1}{2}\dot{q}_5(L_4(\theta_6+\theta_{10}) + \theta_8(L_4-2L_5))\cos(q_5)
\end{aligned}
$$

$$
\begin{aligned}
C_{3,4} &= (\frac{1}{2}(\theta_8+\theta_{10}+\theta_6)\cos(2q_4+q_5)+\theta_{10}\cos(2q_5+2q_4))L_4 \\
&\quad \times(\dot{q}_4+\dot{q}_5)-\frac{1}{2}(\dot{q}_4+\dot{q}_5)(L_5L_4\theta_{12}+(2L_5-L_4)(\theta_7+L_6\theta_{12}) \\
&\quad +\theta_{11}L_5L_4+L_4(\theta_9-\theta_5))\sin(q_5)+\frac{1}{2}L_4(\dot{q}_4+\dot{q}_5)((L_5+L_6)\theta_{12} \\
&\quad +\theta_7+L_5\theta_{11}+\theta_5+\theta_9)\sin(2q_4+q_5) \\
&\quad +\frac{1}{2}L_4(\dot{q}_4+\dot{q}_5)((2L_5-L_4)(\theta_{12}+\theta_{11})+2\theta_9)\sin(2q_5+2q_4) \\
&\quad +\frac{1}{2}(\dot{q}_4+\dot{q}_5)((2L_5-L_4)\theta_8-L_4(\theta_{10}+\theta_6))\cos(q_5)
\end{aligned}
$$

$$
\begin{aligned}
C_{4,2} &= \dot{q}_2 d_{2\_0'}((L_5-L_4)(\theta_{12}+\theta_{11})+\theta_9)\cos(q_4+q_5) \\
&\quad +\frac{1}{2}\dot{q}_2((L_5-L_4)(L_6\theta_{12}+\theta_7)-L_4\theta_5)\left(\sin(q_5)-\sin(2q_4+q_5)\right) \\
&\quad +\frac{1}{2}\dot{q}_2(2L_4\theta_9-(\theta_{12}+\theta_{11})(L_5-L_4)^2)\sin(2q_5+2q_4) \\
&\quad +\dot{q}_2L_4\theta_{10}\cos(2q_5+2q_4)-\dot{q}_2 d_{2\_0'}\theta_{10}\sin(q_4+q_5) \\
&\quad +\frac{1}{2}\dot{q}_2(L_4\theta_6-(L_5-L_4)\theta_8)(\cos(q_5)+\cos(2q_4+q_5))
\end{aligned}
$$

$$
\begin{aligned}
C_{4,3} &= \frac{1}{2}\dot{q}_4(L_4(\theta_9-\theta_5+\theta_{11}L_5)+(2L_5L_6-L_6L_4+L_5L_4)\theta_{12} \\
&\quad +(2L_5-L_4)\theta_7)\sin(q_5)+L_4(\dot{q}_4+\dot{q}_5)\theta_{10}\cos(2q_5+2q_4) \\
&\quad +\frac{1}{2}\dot{q}_4L_4((L_5+L_6)\theta_{12}+\theta_7+L_5\theta_{11}+\theta_5+\theta_9)\sin(2q_4+q_5) \\
&\quad +\frac{1}{2}\dot{q}_4L_4(\theta_8+\theta_6+\theta_{10})\cos(2q_4+q_5) \\
&\quad +\frac{1}{2}L_4(\dot{q}_4+\dot{q}_5)((2L_5-L_4)(\theta_{12}+\theta_{11})+2\theta_9)\sin(2q_5+2q_4) \\
&\quad +\frac{1}{2}\dot{q}_4(L_4(\theta_6+\theta_{10})+\theta_8(L_4-2L_5))\cos(q_5)
\end{aligned}
$$

$$
\begin{aligned}
C_{4,4} &= \frac{1}{2}L_4(\dot{q}_4+\dot{q}_5)((2L_5-L_4)(\theta_{12}+\theta_{11})+2\theta_9)\sin(2q_5+2q_4) \\
&\quad +L_4(\dot{q}_4+\dot{q}_5)\theta_{10}\cos(2q_5+2q_4)
\end{aligned}
$$

Entries of the gravity vector $g(q,\theta)$

The entries of the gravity vector $g(q,\theta)\in\mathbb{R}^4$ as function of the generalized joint coordinates $q=[\ q_1\quad q_2\quad q_4\quad q_5\ ]^T$, the parameters θ_j, $j=1,\dots 32$, listed in table 4, and the acceleration due to gravity $g=9.81\ \mathrm{m/s^2}$, are given by

$$
g_1 = g_2 = 0
$$

$$
\begin{aligned}
g_3 &= -g(\theta_9+\theta_{12}L_5+L_5\theta_{11})\sin(q_4+q_5)-g(\theta_6+\theta_8)\cos(q_4) \\
&\quad -g(\theta_5+\theta_{12}(L_6+L_4)+L_4\theta_{11}+\theta_7)\sin(q_4)-g\theta_{10}\cos(q_4+q_5)
\end{aligned}
$$

$$
g_4 = -g(\theta_9+\theta_{12}L_5+L_5\theta_{11})\sin(q_4+q_5)-g\theta_{10}\cos(q_4+q_5)
$$

Entries of the vector of friction forces $F(\dot{q},\theta)$

The friction forces $F(\dot{q},\theta)\in\mathbb{R}^4$ in the transposer robot are model by (13), such that the entries of $F(\dot{q},\theta)$ can be written as function of the generalized joint velocities $\dot{q}=[\ \dot{q}_1\quad \dot{q}_2\quad \dot{q}_4\quad \dot{q}_5\ ]^T$ and the parameters θ_j, $j=1,\dots 32$, listed in table 4, as follows

$$
f_1(\dot{q}_1)=\theta_{13}\dot{q}_1+\theta_{17}\left(1-\frac{2}{1+e^{2\theta_{25}\dot{q}_1}}\right)+\theta_{21}\left(1-\frac{2}{1+e^{2\theta_{29}\dot{q}_1}}\right)
$$

$$f_2(\dot{q}_2) = \theta_{14}\dot{q}_2 + \theta_{18}\left(1 - \frac{2}{1+e^{2\theta_{26}\dot{q}_2}}\right) + \theta_{22}\left(1 - \frac{2}{1+e^{2\theta_{30}\dot{q}_2}}\right)$$

$$f_3(\dot{q}_4) = \theta_{15}\dot{q}_4 + \theta_{19}\left(1 - \frac{2}{1+e^{2\theta_{27}\dot{q}_4}}\right) + \theta_{23}\left(1 - \frac{2}{1+e^{2\theta_{31}\dot{q}_4}}\right)$$

$$f_4(\dot{q}_5) = \theta_{16}\dot{q}_5 + \theta_{20}\left(1 - \frac{2}{1+e^{2\theta_{28}\dot{q}_5}}\right) + \theta_{24}\left(1 - \frac{2}{1+e^{2\theta_{32}\dot{q}_5}}\right)$$

Acknowledgments

The first author acknowledges support from the National Council for Science and Technology (CONACyT), Mexico, scholarship number 72368

References

[1] Armstrong-Hélouvry, B., 1991, *Control of Machines with Friction*, Kluwer Academic Publishers, Boston.

[2] Armstrong-Hélouvry, B., Dupont, P., and Canudas de Wit, C., 1994, "A survey of models, analysis tools and compensation methods for the control of machines with friction", Automatica, **30**, pp. 1083-1138.

[3] Canudas de Wit, C., Olsson, H., Åström, K. J., and Lischinsky, P., 1993, "Dynamic Friction Models and Control Design", proceedings of the American Control Conference, pp. 1920-1926, San Francisco, California.

[4] Calafiore, G., Indri, M., and Bona, B., 2001, "Robot Dynamic Calibration: Optimal Excitation Trajectories and Experimental Parameter Estimation", Journal of Robotic Systems, **18**, pp. 55-68.

[5] Craig, J. J., 1988, *Adaptive Control of Mechanical Manipulators*, Addison Wesley, New York.

[6] Gelb, A., 1996, *Applied Optimal Estimation*, MIT Press, Cambridge, Massachusetts.

[7] Hensen, R. H. A., G. Z. Angelis, M. J. G. v. d. Molengraft, A. G. de Jager, and J. J. Kok, 2000, "Grey-box modeling of friction: An experimental case-study", European Journal of Control, **6**, pp. 258-267.

[8] Kostic D. , R. Hensen, B. de Jager, and M. Steinbuch, 2001, "Modeling and identification of an RRR-robot", Proceedings of the IEEE Conference on Decision and Control, pp. 1144-1149.

[9] Lee, C. S. G., 1982, "Robot Arm Kinematics, Dynamics and Control", IEEE Computer, **15**, pp. 62-80.

[10] Lewis, F. L., Abdallah, C. T., and Dawson, D. M.,1993, *Control of Robot Manipulators*, Macmillan, New York.

[11] Ljung, L., 1987, *System Identification: Theory for the User*, Prentice Hall, Englewood Cliffs, NJ.

[12] Swevers, J., Granseman, C., Bilgin Tükel., D., and De Schutter J., 1997, "Optimal Robot Excitation and Identification", IEEE, Transactions on Robotics and Automation, **13**, pp. 730-740.

[13] *Servo Motor Amplifiers DCPA 50/2 and DCPA 50/2D, Document Ref. 8122 968 5029.0*, Phillips CFT Engineering, Eindhoven, The Netherlands, 1994.

[14] *DC ServoMotors series* RX, PARVEX S.A., France, 1999.

[15] Spong, M. W., and Vidyasagar, M., 1989, *Robot Dynamics and Control*, John Wiley & Sons, Inc., New York.